Repeated near-collapse of the Pliocene sea surface temperature gradient in the North Atlantic

B.D.A. Naafs[1,2], A.H.L. Voelker[3,4], C. Karas[5,6,7,8], N. Andersen[9], F.J. Sierro[10]

[1]Organic Geochemistry Unit, School of Chemistry and Cabot Institute, University of Bristol, Bristol, UK
[2]School of Earth Sciences, University of Bristol, Bristol, UK
[3]Divisão de Geologia e Georecursos Marinhos, Instituto Português do Mar e da Atmosfera, Lisboa, Portugal
[4]CCMAR, Centro de Ciências do Mar, Universidade do Algarve, Campus de Gambelas, Faro, Portugal
[5]Goethe-University Frankfurt, Altenhoeferallee 1, 60438, Frankfurt am Main, Germany
[6]Lamont-Doherty Earth Observatory, Geoscience, Palisades, USA
[7]Instituto de Geografía, Pontificia Universidad Católica de Chile, Santiago, Chile
[8]Millennium Nucleus Paleoclimate, University of Chile, Santiago, Chile
[9]Leibniz Laboratory for Radiometric Dating and Stable Isotope Research, CAU Kiel, Kiel, Germany
[10]Department of Geology, Faculty of Sciences, University of Salamanca, Salamanca, Spain

1. Abstract

Sea surface temperature (SST) are used to infer past changes in the state of the climate system. Here we use a combination of newly generated and published organic paleothermometer records, together with novel high-resolution benthic foraminiferal $\delta^{18}O$ stratigraphy, from four sites in the mid-latitude North Atlantic (41-58 °N) to reconstruct the long-term evolution of the latitudinal SST gradient during the Pliocene and early Pleistocene (4.0 to 2.4 Myr), the last time atmospheric CO_2 reached concentrations above 400 ppmv. We demonstrate that the latitudinal SST gradient in the North Atlantic nearly collapsed twice during this period. We conclude that the latitudinal SST gradient in the mid-latitude North Atlantic has two end-members; a maximum as existing at present and a minimum that existed during certain periods of the (late) Pliocene. Our results suggest that the 400 ppmv Pliocene world was much more dynamic than currently thought.

2. Introduction

During the Pliocene epoch (5.33 to 2.59 Myr) concentrations of atmospheric CO_2 ranged from 240 to 450 ppmv (Seki et al., 2010; Bartoli et al., 2011; Martinez-Boti et al., 2015). The Pliocene can therefore provide valuable insights into the climate state of a 400 ppmv world. In addition, the paleogeography during the Pliocene was relatively similar to today, especially during the late Pliocene. However, a few important ocean gateways such as the Central American Seaway (CAS) and the Bering Strait opened during the Pliocene and might have impacted climate circum the North Atlantic (Haug and Tiedemann, 1998; Horikawa et al., 2015). Over the past decades a lot of focus has been on the period 3.260-3.025 Myr, known as the mid-Piacenzian warm period (mPWP) or Pliocene Research Interpretation and Synoptic Mapping (PRISM) interval (e.g., Dowsett et al., 1992; Dowsett et al., 2012; Haywood et al., 2016). Proxy reconstructions indicate that (especially interglacial) sea surface temperatures (SSTs) were higher than at present during this ~ 235 kyr period, especially at the higher latitudes in the North Atlantic, leading to a reduced latitudinal SST gradient (Dowsett et al., 1992; Dowsett et al., 2012). A warming of the climate system is also recorded in the terrestrial realm from the middle to late Pliocene (e.g., Salzmann et al., 2013). Although there have been some recent advances (Otto-Bliesner et al., 2017), climate models generally underestimate the extent of surface ocean warming during the mPWP in the northern North Atlantic as indicated by proxy records (Haywood et al., 2016).

During the Holocene, Northern Hemisphere temperature gradients have been shown to influence precipitation patterns and storm tracks due to changes in atmospheric dynamics such as a reduction in the strength of the westerlies and jets (Shaw et al., 2016; Routson et al., 2019). For the Pliocene variations in SST gradients have been linked to changes in ocean circulation and overturning (Dowsett et al., 1992), upwelling (Arnold and Tziperman, 2016), atmospheric circulation and the hydrological cycle (Burls and Fedorov, 2017), and continental ice sheet inception (Brierley and Fedorov, 2010). For example, Brierley and Fedorov (2010) used climate model simulations to show that increasing SST gradients for the Pliocene led to changes in atmospheric deep convection and cloud cover that triggered cooling and an increase in snowfall over North America.

However, although SST gradients play an important role in the climate system, besides a few exceptions that focus on the brief mPWP/PRISM period around 3 Myr (Robinson et al., 2008; Dowsett et al., 2012) or warm Pliocene period (Lawrence et al., 2009; Bachem et al., 2017), the long-term evolution of the latitudinal SST gradient in the North Atlantic during the Pliocene is poorly constrained. For example, its evolution across the intensification of Northern Hemisphere Glaciation (~ 3.0-2.5 Myr) is not well known, hindering a holistic assessment of the mechanisms that drove this major climatic transition. Although local and small continental ice sheets and sea ice might have existed in the high-Arctic since the Eocene/Oligocene (e.g., Jansen and Sjøholm, 1991; Eldrett et al., 2007; Krylov et al., 2008), the occurrence of ice-rafted debris across the North Atlantic around 2.7-2.5 Myr (Shackleton et al., 1984; Bailey et al., 2013; Naafs et al., 2013b) and simultaneous onset of seasonal sea-ice cover in the northern North Atlantic (Knies et al., 2014) marked the onset of larger glacial-interglacial cycles with the episodic appearance of large continental ice sheets on Greenland, North America, and Scandinavia. Here we use a combination of organic geochemical temperature proxies to provide new insights into the long-term evolution of the latitudinal SST gradient in the mid-latitude North Atlantic (41-58 °N) from 4.0 to 2.4 Myr, spanning the transition from the warm Pliocene into the Pleistocene and the intensification of Northern Hemisphere Glaciation.

3. Chronologies

For Integrated Ocean Drilling Program (IODP) Site U1313 and Deep Sea Drilling Program (DSDP) Sites 610 and 609 we updated the existing age models using published and newly generated benthic foraminiferal $\delta^{18}O$ data. For Ocean Drilling Program (ODP) Site 982 we used the published age model (Lawrence et al., 2009).

3.1 DSDP Site 610

An initial age model of Site 610A was based on magnetostratigraphic control points (Baldauf et al., 1987). Later work led to more refined (late) Pliocene and early Pleistocene age models, based on benthic foraminiferal $\delta^{18}O$ (Jansen et al., 1988; Raymo et al., 1992; Kleiven et al., 2002). De Schepper and Head (2008) revised the Pliocene part of this age model based on dinoflagellate cyst and acritarch events. These authors revaluated and updated all relevant age control data (e.g. magnetostratigraphy, nannofossil biodatums, benthic isotope data) according to the ATNTS time scale and the LR04 stack (Lisiecki and Raymo, 2005), re-dating the initial age of the base of the core about 1 Ma younger than previous interpretations. This age model was further fine-tuned around the glacial M2 event (De Schepper et al., 2013). However, a high-resolution benthic $\delta^{18}O$ record to refine the age model was not available for the older part of the core (> 3.4 Myr).

We therefore generated a new benthic foraminiferal (*Cibicidoides wuellerstorfi*) $\delta^{18}O$ record for the period 4.0-3.3 Myr using an average temporal resolution of ~4 kyr. Before selecting benthic foraminiferal tests for foraminiferal $\delta^{18}O$, all samples were washed over a 63 µm sieve and separated into different size fractions. Using a binocular microscope, visible clean 2-3 specimens from the 250-315 µm size fraction were selected and subsequently analyzed on a Thermo Scientific MAT-253 equipped with a Gas Bench II (Frankfurt University). Precision was better than ± 0.08 ‰. The reported values are relative to Vienna Pee Dee Belemnite (VPDB, based on the National Bureau of Standards standard NBS-19).

We combined our new high-resolution benthic $\delta^{18}O$ record during the time period ~3.3-4 Ma together with published data from 3.3-2.4 Myr (Jansen et al., 1988; Raymo et al., 1992; Kleiven et al., 2002; De Schepper et al., 2013) to create a high-resolution age model over the period from 4-2.4 Myr. Our data is consistent with $\delta^{18}O$ data from the same species and Site (De Schepper et al., 2013). However, published benthic foraminiferal $\delta^{18}O$ data from the genus Cibicides spp. spanning the depth interval between 180 and 162 mcd (~3.6 and 3.3 Myr) (Kleiven et al., 2002) show more scatter and overall lower values compared to our new benthic foraminiferal $\delta^{18}O$ data (from species *C. Wuellerstorfi*; Fig. S1). As the reduced amplitude of variability in our record compared to that in the Kleiven et al. (2002) dataset is more consistent with that observed in the global LR04 stack (Lisiecki and Raymo, 2005) we did not included the Kleiven et al. (2002) $\delta^{18}O$ data for the depth interval between 180 and 162 mcd (~3.6 and 3.3 Myr). The final age model was obtained by (peak) tuning the benthic foraminiferal $\delta^{18}O$ data from Site 610A to the global LR04 benthic $\delta^{18}O$ stack (Lisiecki and Raymo, 2005), also taking the magnetostratigraphy and biodatums into account (Fig. 2).

3.2 DSDP Site 609

Originally tuned to the benthic $\delta^{18}O$ record from ODP Site 846, we updated the age model for Hole 609B by retuning the available benthic $\delta^{18}O$ data from 3.4-2.75 Myr (Bartoli et al., 2005) to the global LR04 benthic $\delta^{18}O$ stack (Lisiecki and Raymo, 2005) (Fig. 3).

3.3 IODP Site U1313

Site U1313 is a re-drill of DSDP Site 607. Between 3.3 and 2.4 Myr, we used the published age model for Site U1313, based on tuning the lightness (L*) of Site U1313 to the carbonate content of DSDP Site 607, part of the LR04 benthic isotope stack, as well as directly to the LR04 stack (Expedition 306 Scientists, 2006; Naafs et al., 2011; Naafs et al., 2012a). This age model provides a close correlation between the published benthic foraminiferal $\delta^{18}O$ data from Site U1313 (Bolton et al., 2010; De Schepper et al., 2013) (Fig. S4) and the LR04 benthic isotope stack for this interval (Fig. 4). We prefer to use the lightness-based age model for the 3.3-2.4 Myr interval as this is based on correlating signals from the same location (L* from

Site U1313 to $CaCO_3$ from Site 607) and not to a global signal like LR04 where signals might be smoothed out. Because the variations in lightness are reduced beyond 3.3 Myr, for the interval between 4.3-3.3 Myr a new high-resolution benthic foraminiferal $\delta^{18}O$ record was generated using the primary splice.

New stable isotope data was obtained using a 5-cm sampling resolution (Lisbon series) spanning the interval from 157.21 to 190.21 adjusted meter composite depth (amcd) (for details on the amcd, see Naafs et al., 2012a). 680 samples were prepared following the established procedure in the Sedimentology and Micropaleontology laboratory of IPMA (Instituto Português do Mar e da Atmosfera). After freeze drying, each sediment sample was washed through a 63 µm-mesh using deionized water. The coarse fraction was dried in filter paper at 40 °C and weighed. After dry sieving, 2-6 clean specimens of the benthic foraminifer species *Cibicidoides wuellerstorfi*, *Cibicidoides mundulus* or *Cibicidoides* sp. were selected from the fraction > 250µm for stable isotope analyses. In rare instances specimens from more than 1 species were combined for analysis. The Lisbon-series samples were analyzed at MARUM, University Bremen (Germany). The samples were measured using Finnigan MAT 251 mass spectrometers, coupled to an automated Kiel I or Kiel III carbonate preparation system. The mass spectrometers' long-term precision is ± 0.07 ‰ for $\delta^{18}O$ based on repeated analyses of internal (Solnhofen carbonate) and external (NBS-19) carbonate standards. Based on this newly analyzed isotope data, a discrepancy in the primary splice was encountered between 176 and 182 amcd. Using the benthic foraminiferal $\delta^{18}O$ data and lightness (L*) record, we corrected the splice by inserting 1.9 m of sediments from sections U1313B-18H-1 and U1313B-18H-2 into the splice and subsequently shifting all amcd depths starting with Cores U1313B-18H and U1313C-19H (Fig. S2).

In addition, 240 samples were prepared for benthic foraminiferal $\delta^{18}O$ from the interval 150-201 amcd at the University of Salamanca (Salamanca series). All these samples were disaggregated with tap water, sieved through 62 and 150 µm sieves, dried and weighed. For isotope analyses 1 to 5 specimens of *Cibicidoides wuellerstorfi* were picked from the 250-500 µm fraction. Specimens were washed with methanol, ultrasonicated for several seconds and dried at room temperature for 24 hours. The stable isotopic composition was analyzed at the Leibniz Laboratory for Radiometric Dating and Stable Isotope Research (Kiel University, Germany) using a Kiel IV carbonate preparation device connected to a MAT 253 mass spectrometer from ThermoScientific. All values are reported in the Vienna Pee Dee Bee notation (VPDB) relative to NBS19. Precision is < 0.09 ‰ for $\delta^{18}O$. The final age model was obtained by tuning the new benthic $\delta^{18}O$ data for the 4.3-3.3 Myr interval to the global LR04 benthic $\delta^{18}O$ stack (Lisiecki and Raymo, 2005) and combining this with the lightness-based age model for the 3.3-2.4 Myr interval (Fig. 4).

4. Analytical methods for SST analyses

To reconstruct SSTs we predominantly used the modified alkenone paleothermometer; U^{K}_{37}' (Brassell et al., 1986; Prahl and Wakeham, 1987), which is commonly applied to the Pliocene (e.g., Lawrence et al., 2009; Herbert et al., 2010; Naafs et al., 2010; Fedorov et al., 2013). We studied a transect of four sites (Fig. 1). This consists of previously published SST data from ODP Site 982 (Lawrence et al., 2009), which is located at 58 °N. We generated a new U^{K}_{37}'-based SST record for DSDP Site 610 (53 °N) that spans the period 4.0-2.2 Myr, supplemented by previously published U^{K}_{37}'-based SST data from the brief interval around marine isotope stage (MIS) M2 (De Schepper et al., 2013). We extended the previously published U^{K}_{37}'-based SST record from IODP Site U1313 (41 °N) that spanned the period from 3.7-2.4 Myr (Naafs et al., 2010) back to 4.3 Myr. Lastly, we provided new U^{K}_{37}'-based SST data from DSDP Site 609 (49.5 °N) for the interval 2.93 - 2.77 Myr and combined this with the existing U^{K}_{37}' data from the period 3.3-2.95 Myr (Robinson et al., 2008). For Site 610 we also generated a second SST record using the independent TEX_{86} SST proxy (Schouten et al., 2002).

4.1 DSDP Site 610

83 new samples from Site 610A between 112 and 199 meter composite depth (mcd) were used for organic geochemical analyses at the Organic Geochemistry Unit (OGU) in Bristol. The average sample resolution is ~ 20 kyr. The samples were frozen and subsequently dried in a freeze-dryer to remove excess water and then crushed to a fine powder using a pestle and mortar. Lipids were obtained using a Milestone Ethos Ex microwave extraction system. For this purpose approximately 5 gram of sediment and 10 ml of a mixture of dicloromethane (DCM) and methanol (MeOH) (9:1, v/v) was used. The microwave program consisted of a 10 min ramp to 70 °C (1000 W), 10 min hold at 70 °C (1000 W), and 20 min cool down. The samples were then centrifuged for 5 minutes (1500 rounds per minute). The supernatant fluid was removed, after which 10 ml of DCM:MeOH (9:1) was added to the remaining sediment and the samples centrifuged again. This process was repeated three times to ensure that all extractable organic matter was obtained. The total lipid extract (TLE) was subsequently dried using rotary evaporation to near-dryness and then dried to completeness using N_2.

The relative abundance of C_{37} alkenones was determined using a Hewlett Packard 5890 Series II gas chromatograph coupled to a flame ionization detector (GC-FID). Prior to analysis by GC-FID the TLE was derivatised by adding 50 µl of pyridine and 40 µl of BSTFA (bis-(trimethylsilyl)trifluoroaceamide) to each sample and subsequently heated at 70 °C for 1 hour. Derivatized samples were analyzed by GC-FID within 24 hours. The GC-FID was equipped with a Restek Rtx-1 column (50 m long x 0.32 mm internal diameter x 0.17 µm film thickness). Injection volume was 1 µl. The oven programme was: 70 °C (1 min hold) to 130 °C at 20 °C/min, then to 300 °C (held 24 min) at 4 °C/min. Replicate analyses (n= 20) of an in-house alkenone standard indicated that the standard deviation of the U^{K}_{37}' measurements was < 0.01, approximately < 0.3 °C.

The relative abundance of glycerol dialkyl glycerol tetraethers (GDGTs) was analyzed using a high performance liquid chromatography-atmospheric pressure ionization-MS (HPLC-APCI-MS) with a ThermoFisher Scientific Accela Quantum Access triple quadrupole MS instrument. For this purpose the TLE was re-dissolved in hexane/*iso*-propanol (99:1, v/v) and passed through a 0.45 µm PTFE filter prior to analysis by HPLC-APCI-MS. Injection volume was 15 µl. Normal phase separation was achieved with an Alltech Prevail Cyano column (150 mm x 2.1 mm x 3 µm) at a flow rate of 200 µl/min. The initial solvent was hexane/*iso*-propanol 99:1 (v/v), eluted isocratically for 5 min, followed by a linear gradient to 1.8% *iso*-propanol over 45 min. Selective ion monitoring (SIM) was used, scanning for both isoprenoid (*iso*) and branched (*br*) GDGTs, to increase sensitivity and reproducibility and $\{M+H\}^+$. GDGT peaks were integrated (*m*/*z* 1302, 1300, 1298, 1296, 1294 and 1292 for *iso*GDGTs, and *m*/*z* 1050, 1036, 1034, 1032, 1022, 1020, 1018 for *br*GDGTs). Long-term analysis of an in-house marine GDGT standards indicated that the standard deviation of the TEX_{86} measurements was <0.05 (< 2 °C).

4.2 DSDP Site 609

22 new samples from Hole 609B between 200.8 and 185.3 meter composite depth (mcd) were used for organic geochemical analyses at the OGU in Bristol. The average sample resolution is ~ 8 kyr. We followed the same procedure as explained above for Site 610. The only difference is that for Site 609 the samples were analyzed using a Thermo Scientific Trace 1300 GC-FID system. Injection volume was 1 out of 30 µl. The column type and GC-oven program were the same as used to analyze the samples from Site 610. Replicate analyses of the inhouse alkenone standard indicated that the standard deviation of the U^{K}_{37}' measurements is < 0.01, representing < 0.3 °C.

4.3 IODP Site U1313

We extended the previously published alkenone-based SST record from Site U1313 (Naafs et al., 2010; Naafs et al., 2012a) back to 4.3 Myr. This work was done at the Alfred Wegener Institute (AWI). For this purpose 121 additional samples from between 175 and 200 amcd of the primary splice of Site U1313 were taken at a sampling interval of 20 cm (~4 kyr). Sample preparation for the organic geochemical analysis followed the procedures explained in Naafs et al. (2010; 2012a). Samples were freeze-dried and homogenized using a mortar and pestle. Around 5 gram of sediment was extracted using dichloromethane and accelerated solvent extraction (ASE 200, DIONEX, 5 min. at 100 °C and 1000 psi). The TLE was concentrated using rotary evaporation and dried to completeness using N_2. The TLE was re-dissolved in 500 µl of hexane. The U^{K}_{37}’ was determined using a LECO Pegasus III gas chromatograph coupled to a time of flight mass spectrometer (GC/TOF-MS) at AWI, following the methods explained in Hefter (2008). Long-term analysis of an extract of an *E. huxleyi* culture shows that the standard deviation of the U^{K}_{37}’ measurements is << 0.01, representing an error of < 0.2 °C.

5. SST proxies and calibrations

5.1 Modified alkenone unsaturation index of long-chain ketones (U^{K}_{37}’)

Over the last decade a wide-range of studies have successfully applied the alkenone paleothermometer to Pliocene samples from the North Atlantic (e.g., Robinson et al., 2008; Lawrence et al., 2009; Lawrence et al., 2010; Naafs et al., 2010; Dowsett et al., 2012; Fedorov et al., 2013; Bachem et al., 2017). We used the modified alkenone unsaturation index of long-chain ketones (U^{K}_{37}’) (Brassell et al., 1986; Prahl and Wakeham, 1987). To convert the U^{K}_{37}’ data to SST for all sites (including the published data from Site 982), the global core-top calibration was used (Müller et al., 1998). This calibration provides mean annual temperatures at the surface (top 10 meters of the water column).

$$U^{K'}_{37} = \frac{[C_{37:2}\ alkenone]}{[C_{37:2}\ alkenone] + [C_{37:3}\ alkenone]}$$

$U_{37}^{K}{}' = 0.033 \times SST + 0.044\ (r^2 = 0.96, n = 370, st.dev = 1.5\ ℃)$

The error bars shown for the alkenone-based SSTs reflect the combined uncertainty of the calibration (1.5 °C (Müller et al., 1998)) and analytical uncertainty (~0.3 °C) using:

$Combined\ uncertainty = \sqrt{1.5^2 + 0.3^2} = 1.5\ ℃$.

5.2 Tetraether index of tetraethers consisting of 86 carbon atoms (TEX_{86})

In addition to the alkenone paleothermometer, a number of studies, predominantly focusing on the western Pacific warm-pool, have applied the tetraether index of tetraethers consisting of 86 carbon atoms (TEX_{86}) (Schouten et al., 2002) to reconstruct sea surface temperatures during the Pliocene (e.g., O'Brien et al., 2014; Zhang et al., 2014). We applied this method to provide additional and independent SST estimates from DSDP Site 610. The recently developed BAYSPAR deep time analogue calibration was used to convert TEX_{86} to SST (Tierney and Tingley, 2014, 2015). The deep-time model of BAYSPAR selects TEX_{86} values from the modern dataset (n = 1095) with a similar TEX_{86} value to that of the paleorecord and then uses these to construct a linear regression. A prior value of 18 °C and a broad standard deviation of 10 °C was used to select the best calibration. The search tolerance was 0.1 (2σ of the inputted TEX_{86} data). The resulting linear calibration is based on “analogue” locations from the (sub)tropics and mid-latitudes. Error bars of the TEX_{86}-based SSTs are the 95% (1σ) confidence intervals.

$$TEX_{86} = \frac{[isoGDGT-2] + [isoGDGT-3] + [cren']}{[isoGDGT-1] + [isoGDGT-2] + [isoGDGT-3] + [cren']}$$

$$TEX_{86} = 0.0144 \times SST + 0.273$$

To assess the contribution of allochthonous (terrestrial) GDGTs that can bias the TEX_{86}-SST proxy, the branched and isoprenoidal tetraether (BIT) index was used (Hopmans et al., 2004).

$$BIT = \frac{[brGDGT-Ia] + [brGDGT-IIa] + [brGDGT-IIIa]}{[brGDGT-Ia] + [brGDGT-IIa] + [brGDGT-IIIa] + [cren]}$$

The BIT index at Site 610 was < 0.4 in most samples, indicating a low contribution of terrestrial GDGTs to the overall GDGT pool. The nine samples with a BIT index > 0.4 were excluded from the SST record.

6. Results

The new alkenone-based SST records from Sites 610 and U1313 indicate a long-term cooling trend across the Pliocene into the Pleistocene. The lower resolution record from Site 610 (Fig. 5) indicates a decline from ~ 22 °C around 4 Myr to ~14 °C (minima of 8.5 °C) during peak glacials after 2.7 Myr. This long-term alkenone-based SST evolution of cooling at Site 610 is confirmed by the TEX_{86} record. However, the magnitude of cooling is less in the TEX_{86} compared to the alkenone-based SST record because the minimal SSTs during intense Pleistocene glacials are higher in the TEX_{86} record, never reaching < 12 °C.

The alkenone-based record from Site U1313 (Fig. 6) indicates a SST decline from ~ 22 °C around 4.2 Myr to < 16 °C during peak glacials after 2.7 Myr. The shorter SST record from Site 609 indicates temperatures of 16-20 °C from 3.3 to 2.8 Myr with no clear long-term trend (Fig. 7).

7. Discussion

7.1 Comparison with planktonic foraminiferal Mg/Ca-based SST estimates from Sites U1313, 609, and 610

Besides the U^{K}_{37}'- and TEX_{86}-based SSTs records that we generated, a number of (shorter) records (predominantly based on planktonic foraminiferal Mg/Ca) exist for Sites U1313/607, 610, and 609. Most of these Mg/Ca records do not allow for the assessment of the long-term temperature trends observed in our records as they only span parts of our long-term record, predominantly the interval 3.3-2.4 Myr. However, they can provide insights into whether the U^{K}_{37}'- (and TEX_{86}-based) temperatures are consistent with those obtained using other proxies.

The comparison between organic and inorganic SSTs records at Site U1313 (and its precursor Site 607) has been discussed previously and indicates a general good agreement between *G. bulloides* Mg/Ca and U^{K}_{37}'-based SSTs in terms of trends and absolute values during the 3.3-2.4 Myr interval (Robinson et al., 2008; De Schepper et al., 2013; Friedrich et al., 2013; Hennissen et al., 2014, 2017). The same was found for Site 609 for the interval between 3.3-3.0 Myr (Robinson et al., 2008). Also, a brief SST record from U1313 that spans MIS 98-96 (~2.4 Myr) obtained using the independent long-chain diol index indicates a good agreement with U^{K}_{37}'-based SSTs (Naafs et al., 2012b). On the other hand, *G. ruber* Mg/Ca based SSTs from U1313/607 and 609 are generally slightly higher and characterized by a dampened glacial/interglacial variability compared to SSTs based on *G. bulloides* Mg/Ca and U^{K}_{37}' (Robinson et al., 2008; Friedrich et al., 2013; Hennissen et al., 2014). This offset between *G. ruber* Mg/Ca based SSTs and those obtained using *G. bulloides* Mg/Ca and U^{K}_{37}' that is observed for the 3.3-2.4 Myr interval has been related to *G. ruber* reflecting warm season temperatures and not mean annual (e.g., Robinson et al., 2008).

Site 610 is the only site in the North Atlantic where multiple SSTs records exist that span the majority of the 4-2.4 Myr interval (Fig. 5). The U^{K}_{37}' and TEX_{86}-based SSTs that we generated are in good agreement with each other in terms of absolute values and trends. The tropical planktonic foraminifera *G. ruber* is not found at Site 610 during the Plio/Pleistocene, but *G. bulloides* Mg/Ca based SSTs are available for the interval between 4-3.2 Myr (De Schepper et al., 2013; Karas et al., 2020) and 2.8-2.5 Myr (Hennissen et al., 2014). As observed at Sites U1313 and 609, for the latest Pliocene interval the *G. bulloides* Mg/Ca-based SSTs are in relatively good agreement with U^{K}_{37}' (and TEX_{86})-based SSTs, but 3-4 °C lower during MIS G9-G7 (~2.75 Myr). Although the overall cooling trend in the *G. bulloides* Mg/Ca-based SSTs for the 4-3.2 Myr interval is similar as that seen in the organic-based SSTs, the absolute SSTs are consistently 3-4 °C lower. The observation that the two independent organic proxies (U^{K}_{37}' and TEX_{86}) give similar SSTs, gives us confidence that these SSTs are robust. The divergence of the Mg/Ca-based SSTs could be related to *G. bulloides* having a different (deeper) depth habitat during the early Pliocene or is reflecting a Spring bloom temperature signal (see also discussion in Karas et al., 2020). However, there is no evidence for a shift in depth habitat or bloom period of *G. bulloides* across the Pliocene. Alternatively, the Mg/Ca-based SSTs for the early Pliocene could be biased by a change in the Mg/Ca of seawater; $(Mg/Ca)_{sw}$. All planktonic foraminiferal Mg/Ca-based SSTs are calculated assuming that $(Mg/Ca)_{sw}$ has remained constant (De Schepper et al., 2013; Hennissen et al., 2014; Karas et al., 2020). However, although $(Mg/Ca)_{sw}$ is constant on 10^3-10^5 yr timescales, there is evidence that $(Mg/Ca)_{sw}$ increased across the Pliocene (e.g., Evans and Müller, 2012). Assuming lower $(Mg/Ca)_{sw}$ during the early Pliocene (> 3.2 Myr) would results in higher *G. bulloides* Mg/Ca based SSTs. However, at this point the exact evolution of $(Mg/Ca)_{sw}$ across the Pliocene is not constrained enough to allow us to correct the Mg/Ca-based SSTs. We speculate that the long-term Mg/Ca-based cooling trend at Site 610 is dampened compared to that recorded by the organic proxies due to long-term changes in $(Mg/Ca)_{sw}$, as suggested for Pliocene Mg/Ca records from the Pacific (O'Brien et al., 2014). Future research should explore the full impact of changes in Pliocene $(Mg/Ca)_{sw}$ on the long-term temperature evolution.

7.2 Comparison with SST records from across the North Atlantic

The long-term cooling trends across the Pliocene recorded at Sites 610 and U1313 (Fig. 5 and 6) are consistent with the trends in other alkenone (Herbert et al., 2016) and Mg/Ca-based SST records (Karas et al., 2017) from the North Atlantic. The alkenone-based cooling between 4 and 2.4 Myr is larger at Site 610 (~ 8 °C) compared to Site U1313 (~ 3 °C). Our interpretation is that during the early Pliocene Site 610 was influenced by warm subtropical waters transported by the NAC, similar to U1313. Between ~3.6 Myr and 2.9 Myr the SST record from Site 610 is on average 2 °C colder than that from Site U1313 reflecting less NAC influence at Site 610 compared to Site U1313 (Karas et al., 2020). After 2.9 Myr, especially during glacials, Site 610 became 4-5 °C colder than Site U1313, reflecting a further reduction in NAC influence at Site 610. From 2.9 Myr onwards the SSTs at Site 610 are similar to those at Site 982 (Fig. 8), which is influenced by colder subpolar waters, suggesting a strongly reduced influence of the NAC at Site 610. Consistent with this, dinoflagellate assemblages from Site 610 record a southward shift of the NAC to a location south of Site 610 at ~ 2.6 Myr (Hennissen et al., 2014).

Following Hodell and Channell (2016) that used the records from 3.2 to 0 Myr, here we calculated the latitudinal SST gradient in the mid-latitude North Atlantic from 4.0 to 2.4 Myr using our extended record from Site U1313 and the existing record from Site 982 (Lawrence et al., 2009) (Fig. 8). We perceive Site 982 to reflect a high-latitude endmember on the northern edge of the region that can be influenced by the NAC and Site U1313 as mid-latitude endmember. For this purpose, the two SST records were resampled at 4 kyr resolution. The two resampled records were subtracted and a 100 kyr moving average of this difference is shown (Fig. 8). It is important to note that this gradient reflects long-term (> 10-100 kyr) changes and may not capture the full (glacial/interglacial) variability during the Plio/Pleistocene.

The gradient has a maximum of 5 °C during the Pliocene/early Pleistocene, less than the modern difference in annual mean temperature of ~7.5 °C based on instrumental observations. However, this Pliocene maximum is similar to the average reconstructed U^{K}_{37}'-based SST gradient for the Holocene (last 10 kyr). Although alkenone-based SSTs at Site U1313 for the Holocene (Naafs et al., 2013a) are similar to the modern instrumental annual mean SST at this location, at Site 982 the alkenone-based SSTs for the Holocene (Lawrence et al., 2009) are ~3 °C higher than modern instrumental annual mean. This likely reflects a bias of the modern alkenone-producers to the warmer season in the more northern Site 982. Consistent with this, a number of studies have found that modern U^{K}_{37}'-based SSTs from the (northern) North Atlantic are influenced by seasonality (Rosell-Melé and Prahl, 2013; Filippova et al., 2016; Tierney and Tingley, 2018). If the Pliocene record from Site 982 is biased towards the warmer season (summer) this means that our reconstructed Pliocene latitudinal SST gradient between Sites 982 and U1313 presents a minimum estimate.

Either way, our results demonstrate that the gradient was not stable and varied across the Pliocene. This result is similar to that reported by Lawrence et al. (2009) for the period 4.0 to 3.5 Myr, but here we demonstrate that this feature persisted across the intensification of Northern Hemisphere Glaciation. The strongest gradient existed from 3.8-3.6, 3.0-3.2 (mPWP/PRISM interval), and after 2.7 Myr, the latter coinciding with the intensification of Northern Hemisphere Glaciation. Periods with the smallest gradient are centered around 3.4 and 2.9 Myr. The alkenone (and TEX_{86}-based) SST gradient between Sites U1313 and 610 (Fig. 9), is also weak during these two periods, although more variable. The extent of the latitudinal SST gradient between Sites U1313 and 610 increases over time as Site 610 cools more during the Plio/Pleistocene than U1313 (Fig. 8) as the influence of the NAC at Site 610 diminishes, especially during the intense glacials of the late Pliocene and early Pleistocene. The fact that we see a similar response at Site 610 as at Site 982 indicates that the collapse is not a simple result of small changes in the path of the NAC across Site 982 (Lawrence et al., 2009).

During the minima the SST gradient between Sites 982 and U1313 was < 2 °C. A reduced latitudinal SST gradient in the North Atlantic was previously reported for the relatively short mPWP/PRISM interval (e.g., Dowsett et al., 1992; Dowsett et al., 2012) but our results show the gradient was actually lower before and after the mPWP.

The periods of lowest latitudinal gradient are predominantly driven by periods of higher SSTs at Site 982 (and 610). This likely reflects periods of increased northward penetration of the NAC, potentially also indicating periods of intensified Atlantic Meridional Overturning Circulation (AMOC). Conversely, maxima occurred around 3.2-3 Ma and 2.6 Myr, which were mainly a result of cooling at northern located Site 982 (and for the second interval Site 610) due to a weakened influence of the NAC at these sites.

During the minimum SST latitudinal gradient around 3.4 Myr, there is a pronounced warming at ODP Site 907 (69 °N) in the northern North Atlantic (Fig. 8). It remains unclear whether such a warming also occurred during the younger minima observed in our latitudinal SST gradient, because low alkenone concentrations question the reliability of the existing alkenone-based SST record for samples younger than 3.3 Myr (Grimalt et al., 2001; Clotten et al., 2018). At Site 907, alkenone-based SSTs start to increase around 3.5 Myr and reach a (late) Pliocene maximum of 10-12 °C around 3.4 Myr (Herbert et al., 2016). This period also coincides with dramatic changes in the dinoflagellate composition at Site 907 (Schreck et al., 2013), further emphasizing an overall re-organization of ocean circulation in the Greenland Sea. However, the warming is not recorded in the alkenone-based SST record from Site DSDP 642 in the Norwegian Sea. Site 642 is influenced by the NE branch of the NAC and records low SSTs around 3.4 Myr (Bachem et al., 2017). As a result, the zonal SST gradient between the Greenland (Site 907) and Norwegian (Site 642) Sea was reduced around 3.4 Myr (Bachem et al., 2017), simultaneous with the near collapse of the latitudinal SST gradient (Fig. 9). We interpret this to reflect an increase in surface heat transport into the northern Atlantic due to partially enhanced NAC, warming Site 982. This stronger circulation possibly also supported the distinct warming in the Greenland Sea seen at Site 907 (Fig. 1) as the East Greenland Current likely was reduced (Bachem et al., 2017). At the same time the NE branch of the NAC weakened, leading to lower temperatures seen at Site 642 (Bachem et al., 2017).

7.3 Potential driving mechanisms

The changes in the latitudinal SST gradient are unrelated to changes in atmospheric CO_2 as indicated by proxy records (Seki et al., 2010; Bartoli et al., 2011; Martinez-Boti et al., 2015) which remained variable but relatively stable from 3.2 to 2.8 Myr when the gradient shifted from a maximum to a minimum (Fig. 8). In this context, the long-term cooling recorded by many SST records in the North Atlantic across the Plio- and early Pleistocene (4-2.4 Myr interval) is not matched by a clear decline in CO_2, raising fundamental questions regarding the processes driving SSTs during this period.

Changes in the throughflow of the Central American Seaway (CAS) have been related to changes in the amount of northward heat transport in the North Atlantic with more heat being transported to the high-latitudes (> 50 °N) as the throughflow decreased (Haug and Tiedemann, 1998; Lunt et al., 2008). However, the impact of closing the CAS on temperatures in the higher latitudes of the North Atlantic is contested by recent modeling studies (Brierley and Fedorov, 2016) and the largest changes in throughflow happened before 4 Myr (e.g., Haug and Tiedemann, 1998; Bell et al., 2015), although surface water exchange might have persisted until the early Pleistocene (~2.5 Ma) (Groeneveld et al., 2014). In addition, there is no clear correlation between our latitudinal SST gradient and the sand content at ODP Site 999, indicative of throughflow of the CAS (Haug and Tiedemann, 1998). In fact, low sand content at Site 999 around 3.4 Myr indicates that CAS throughflow was high (which should lead to a reduced northward heat transport), while the latitudinal gradient between Site 982 and U1313 was at a minimum.

Although classically studies have focused on the CAS, other ocean gateways changed during the Pliocene. For example, Brierley and Fedorov (2016) modelled the impact of changes in the Bering Strait on SSTs in the North Atlantic. The timing of the opening of the Bering Strait is debated and ranges from ~7 to 3 Myr ago (e.g., Marincovich and Gladenkov, 1999; Marincovich and Gladenkov, 2001; Gladenkov and Gladenkov, 2004), but recent studies indicate it occurred during the Pliocene (Verhoeven et al., 2011; Horikawa et al., 2015). Model simulations for Pliocene conditions show that changes in the Bering Strait seaway lead to changes in Arctic freshwater budget, which affect AMOC, the NAC, and ultimately impact

SSTs in the high-latitude North Atlantic (Brierley and Fedorov, 2016). Subsequent model studies have confirmed these results that (high-latitude) North Atlantic SSTs are sensitive to changes in the throughflow of the Bering Strait (Feng et al., 2017; Otto-Bliesner et al., 2017). This scenario needs further testing, especially detailed estimates of the timing of the opening of specific gateways such as the Bering Strait, but we speculate that changes in the gateways, potentially the Bering Strait, might have played a role in North Atlantic climate during the Pliocene, leading to the observed changes in latitudinal SST gradient.

Conclusions

We provide a selection of novel orbitally-resolved U^{K}_{37}'- and TEX_{86}-based SST records together with newly generated benthic foraminiferal $\delta^{18}O$ records from marine sediment cores in the North Atlantic spanning the Pliocene and early Pleistocene. Using these records in combination with published records, we demonstrate that during the Pliocene, the last time when atmospheric CO_2 concentrations reached values above 400 ppmv, the latitudinal SST gradient in the mid-latitude North Atlantic was variable on 100 kyrs time scales. At least twice the gradient became greatly reduced with a SST difference between the mid-latitude (41 °N) and northern North Atlantic (57 °N) of 2 °C, compared to a modern gradient of ~ 7.5 °C. The mechanisms driving these variations in latitudinal SST gradient need further testing but they could be related to changes in (Arctic) ocean gateways. Our results suggest that the 400 ppmv Pliocene world was much more dynamic than currently thought.

Acknowledgements

We thank IODP for providing samples. B.D.A.N. received funding through a Rubicon fellowship, awarded by the Netherlands Organisation for Scientific Research (NWO).

Additional funding came from a Royal Society Tata University Research Fellowship. A.V. acknowledges financial support from the Fundação para a Ciência e a Tecnologia (FCT) through grants IF/01500/2014 and UID/Multi/04326/2019. C. Evans is acknowledged for her help with generating the SST data from DSDP Site 610 . A.V. acknowledges the laboratory support of L. Matos, A. Rebotim, and C. Cavaleiro in Lisbon and M. Segl and H. Kuhnert in Bremen. C.K. thanks the German Science Foundation (DFG) (project KA3461/1-2) and the ANID Millennium Science Initiative /Millennium Nucleus Paleoclimate for funding and J. Fiebig and C. Neu for lab assistance. F.J.S. acknowledges project CGL2015-68459-P, funded the Spanish National Science Agency. All data is archived in the Pangaea database (https://doi.org/10.1594/PANGAEA.913056).

References

Arnold, N.P., Tziperman, E., 2016. Reductions in midlatitude upwelling-favorable winds implied by weaker large-scale Pliocene SST gradients. *Paleoceanography* 31, 27-39, doi: 10.1002/2015PA002806

Bachem, P.E., Risebrobakken, B., De Schepper, S., McClymont, E.L., 2017. Highly variable Pliocene sea surface conditions in the Norwegian Sea. *Climate of the Past* 13, 1153-1168, doi: 10.5194/cp-13-1153-2017

Bailey, I., Hole, G.M., Foster, G.L., Wilson, P.A., Storey, C.D., Trueman, C.N., Raymo, M.E., 2013. An alternative suggestion for the Pliocene onset of major northern hemisphere glaciation based on the geochemical provenance of North Atlantic Ocean ice-rafted debris. *Quaternary Science Reviews* 75, 181-194, doi: 10.1016/j.quascirev.2013.06.004

Baldauf, J.G., Thomas, E., Clement, B., Takayama, T., Weaver, P.P.E., Backman, J., Jenkins, G., Mudie, P.J., et al., 1987. Magnetostratigraphic and biostratigraphic synthesis, Deep Sea Drilling Project Leg 94. *Initial Reports of the Deep Sea Drilling Project* 94, 1159-1205

Bartoli, G., Hönisch, B., Zeebe, R.E., 2011. Atmospheric CO_2 decline during the Pliocene intensification of Northern Hemisphere glaciations. *Paleoceanography* 26, PA4213, doi: 10.1029/2010pa002055

Bartoli, G., Sarnthein, M., Weinelt, M., Erlenkeuser, H., Garbe-Schönberg, D., Lea, D.W., 2005. Final closure of Panama and the onset of northern hemisphere glaciation. *Earth and Planetary Science Letters* 237, 33-44, doi: 10.1016/j.epsl.2005.06.020

Bell, D.B., Jung, S.J.A., Kroon, D., Hodell, D.A., Lourens, L.J., Raymo, M.E., 2015. Atlantic Deep-water Response to the Early Pliocene Shoaling of the Central American Seaway. *Scientific Reports* 5, 12252, doi: 10.1038/srep12252

Bolton, C.T., Wilson, P.A., Bailey, I., Friedrich, O., Beer, C.J., Becker, J., Baranwal, S., Schiebel, R., 2010. Millennial-scale climate variability in the subpolar North Atlantic Ocean during the late Pliocene. *Paleoceanography* 25, PA4218, doi: 10.1029/2010PA001951

Brassell, S.C., Eglinton, G., Marlowe, I.T., Pflaumann, U., Sarnthein, M., 1986. Molecular stratigraphy: a new tool for climatic assessment. *Nature* 320, 129-133, doi: 10.1038/320129a0

Brierley, C.M., Fedorov, A.V., 2010. The relative importance of meridional and zonal SST gradients for the onset of the ice ages and Pliocene-Pleistocene climate evolution. *Paleoceanography* 25, PA2214, doi: 10.1029/2009PA001809

Brierley, C.M., Fedorov, A.V., 2016. Comparing the impacts of Miocene–Pliocene changes in inter-ocean gateways on climate: Central American Seaway, Bering Strait, and Indonesia. *Earth and Planetary Science Letters* 444, 116-130, doi: 10.1016/j.epsl.2016.03.010

Burls, N.J., Fedorov, A.V., 2017. Wetter subtropics in a warmer world: Contrasting past and future hydrological cycles. *Proceedings of the National Academy of Sciences*, doi: 10.1073/pnas.1703421114

Clotten, C., Stein, R., Fahl, K., De Schepper, S., 2018. Seasonal sea ice cover during the warm Pliocene: Evidence from the Iceland Sea (ODP Site 907). *Earth and Planetary Science Letters* 481, 61-72, doi: 10.1016/j.epsl.2017.10.011

De Schepper, S., Groeneveld, J., Naafs, B.D.A., Van Renterghem, C., Hennissen, J., Head, M.J., Louwye, S., Fabian, K., 2013. Northern Hemisphere Glaciation during the Globally Warm Early Late Pliocene. *PLoS ONE* 8, e81508, doi: 10.1371/journal.pone.0081508

De Schepper, S., Head, M.J., 2008. Age calibration of dinoflagellate cyst and acritarch events in the Pliocene–Pleistocene of the eastern North Atlantic (DSDP Hole 610A). *Stratigraphy* 5, 137-161

Dowsett, H.J., Cronin, T.M., Poore, R.Z., Thompson, R.S., Whatley, R.C., Wood, A.M., 1992. Micropaleontological Evidence for Increased Meridional Heat Transport in the North Atlantic Ocean During the Pliocene. *Science* 258, 1133-1135, doi: 10.1126/science.258.5085.1133

Dowsett, H.J., Robinson, M.M., Haywood, A.M., Hill, D.J., Dolan, A.M., Stoll, D.K., Chan, W.-L., Abe-Ouchi, A., et al., 2012. Assessing confidence in Pliocene sea surface temperatures to evaluate predictive models. *Nature Climate Change* 2, 365-371, doi: 10.1038/nclimate1455

Eldrett, J.S., Harding, I.C., Wilson, P.A., Butler, E., Roberts, A.P., 2007. Continental ice in Greenland during the Eocene and Oligocene. *Nature* 446, 176-179, doi: 10.1038/nature05591

Evans, D., Müller, W., 2012. Deep time foraminifera Mg/Ca paleothermometry: Nonlinear correction for secular change in seawater Mg/Ca. *Paleoceanography* 27, PA4205, doi: 10.1029/2012PA002315

Expedition 306 Scientists, 2006. Site U1313, in: Channell, J.E.T., Kanamatsu, T., Sato, T., Stein, R., Alvarez Zarikian, C.A., Malone, M.J., Expedition 303/306 Scientists (Eds.), *Proceedings of Integrated Ocean Drilling Program* Integrated Ocean Drilling Program Management International, Inc., College Station TX.

Fedorov, A.V., Brierley, C.M., Lawrence, K.T., Liu, Z., Dekens, P.S., Ravelo, A.C., 2013. Patterns and mechanisms of early Pliocene warmth. *Nature* 496, 43-49, doi: 10.1038/nature12003

Feng, R., Otto-Bliesner, B.L., Fletcher, T.L., Tabor, C.R., Ballantyne, A.P., Brady, E.C., 2017. Amplified Late Pliocene terrestrial warmth in northern high latitudes from greater radiative forcing and closed Arctic Ocean gateways. *Earth and Planetary Science Letters* 466, 129-138, doi: 10.1016/j.epsl.2017.03.006

Filippova, A., Kienast, M., Frank, M., Schneider, R.R., 2016. Alkenone paleothermometry in the North Atlantic: A review and synthesis of surface sediment data and calibrations. *Geochemistry, Geophysics, Geosystems* 17, 1370-1382, doi: 10.1002/2015gc006106

Friedrich, O., Wilson, P.A., Bolton, C.T., Beer, C.J., Schiebel, R., 2013. Late Pliocene to early Pleistocene changes in the North Atlantic Current and suborbital-scale sea-surface temperature variability. *Paleoceanography* 28, 274-282, doi: 10.1002/palo.20029

Gladenkov, A.Y., Gladenkov, Y.B., 2004. Onset of Connections between the Pacific and Arctic Oceans through the Bering Strait in the Neogene. *Stratigraphy and Geological Correlation* 12, 175-187

Grimalt, J.O., Calvo, E., Pelejero, C., 2001. Sea surface paleotemperature errors in UK_{37}' estimation due to alkenone measurements near the limit of detection. *Paleoceanography* 16, 226-232, doi: 10.1029/1999pa000440

Groeneveld, J., Hathorne, E.C., Steinke, S., DeBey, H., Mackensen, A., Tiedemann, R., 2014. Glacial induced closure of the Panamanian Gateway during Marine Isotope Stages (MIS) 95–100 (~2.5 Ma). *Earth and Planetary Science Letters* 404, 296-306, doi: 10.1016/j.epsl.2014.08.007

Haug, G.H., Tiedemann, R., 1998. Effect of the formation of the Isthmus of Panama on Atlantic Ocean thermohaline circulation. *Nature* 393, 673-676, doi: 10.1038/31447

Haywood, A.M., Dowsett, H.J., Dolan, A.M., 2016. Integrating geological archives and climate models for the mid-Pliocene warm period. *Nature Communications* 7, 10646, doi: 10.1038/ncomms10646

Hefter, J., 2008. Analysis of alkenone unsaturation indices with fast gas chromatography/time-of-flight mass spectrometry. *Analytical Chemistry* 80, 2161-2170, doi: 10.1021/ac702194m

Hennissen, J.A.I., Head, M.J., De Schepper, S., Groeneveld, J., 2014. Palynological evidence for a southward shift of the North Atlantic Current at ~2.6 Ma during the intensification of late Cenozoic Northern Hemisphere glaciation. *Paleoceanography* 29, 2013PA002543, doi: 10.1002/2013PA002543

Hennissen, J.A.I., Head, M.J., De Schepper, S., Groeneveld, J., 2017. Dinoflagellate cyst paleoecology during the Pliocene–Pleistocene climatic transition in the North Atlantic. *Palaeogeography, Palaeoclimatology, Palaeoecology* 470, 81-108, doi: 10.1016/j.palaeo.2016.12.023

Herbert, T.D., Lawrence, K.T., Tzanova, A., Peterson, L.C., Caballero-Gill, R., Kelly, C.S., 2016. Late Miocene global cooling and the rise of modern ecosystems. *Nature Geoscience* 9, 843-847, doi: 10.1038/ngeo2813

Herbert, T.D., Peterson, L.C., Lawrence, K.T., Liu, Z., 2010. Tropical Ocean Temperatures Over the Past 3.5 Million Years. *Science* 328, 1530-1534, doi: 10.1126/science.1185435

Hodell, D.A., Channell, J.E.T., 2016. Mode transitions in Northern Hemisphere glaciation: co-evolution of millennial and orbital variability in Quaternary climate. *Climate of the Past* 12, 1805-1828, doi: 10.5194/cp-12-1805-2016

Hopmans, E.C., Weijers, J.W.H., Schefuß, E., Herfort, L., Sinninghe Damsté, J.S., Schouten, S., 2004. A novel proxy for terrestrial organic matter in sediments based on branched and isoprenoid tetraether lipids. *Earth and Planetary Science Letters* 224, 107-116, doi: 10.1016/j.epsl.2004.05.012

Horikawa, K., Martin, E.E., Basak, C., Onodera, J., Seki, O., Sakamoto, T., Ikehara, M., Sakai, S., et al., 2015. Pliocene cooling enhanced by flow of low-salinity Bering Sea water to the Arctic Ocean. *Nature Communications* 6, 7587, doi: 10.1038/ncomms8587

Jansen, E., Bleil, U., Henrich, R., Kringstad, L., Slettemark, B., 1988. Paleoenvironmental changes in the Norwegian Sea and the northeast Atlantic during the last 2.8 m.y.: Deep Sea Drilling Project/Ocean Drilling Program Sites 610, 642, 643 and 644. *Paleoceanography* 3, 563-581, doi: 10.1029/PA003i005p00563

Jansen, E., Sjøholm, J., 1991. Reconstruction of glaciation over the past 6 Myr from ice-borne deposits in the Norwegian Sea. *Nature* 349, 600-603, doi: 10.1038/349600a0

Karas, C., Khélifi, N., Bahr, A., Naafs, B.D.A., Nürnberg, D., Herrle, J.O., 2020. Did North Atlantic cooling and freshening from 3.65–3.5 Ma precondition Northern Hemisphere ice sheet growth? *Global and Planetary Change* 185, 103085, doi: 10.1016/j.gloplacha.2019.103085

Karas, C., Nürnberg, D., Bahr, A., Groeneveld, J., Herrle, J.O., Tiedemann, R., deMenocal, P.B., 2017. Pliocene oceanic seaways and global climate. *Scientific Reports* 7, 39842, doi: 10.1038/srep39842

Kleiven, H.F., Jansen, E., Fronval, T., Smith, T.M., 2002. Intensification of Northern Hemisphere glaciations in the circum Atlantic region (3.5-2.4 Ma) - ice-rafted detritus evidence. *Palaeogeography, Palaeoclimatology, Palaeoecology* 184, 213-223, doi: 10.1016/S0031-0182(01)00407-2

Knies, J., Cabedo-Sanz, P., Belt, S.T., Baranwal, S., Fietz, S., Rosell-Melé, A., 2014. The emergence of modern sea ice cover in the Arctic Ocean. *Nature Communications* 5, doi: 10.1038/ncomms6608

Krylov, A.A., Andreeva, I.A., Vogt, C., Backman, J., Krupskaya, V.V., Grikurov, G.E., Moran, K., Shoji, H., 2008. A shift in heavy and clay mineral provenance indicates a middle Miocene onset of a perennial sea ice cover in the Arctic Ocean. *Paleoceanography* 23, doi: 10.1029/2007pa001497

Laskar, J., Robutel, P., Joutel, F., Gastineau, M., Correia, A.C.M., Levrard, B., 2004. A long-term numerical solution for the insolation quantities of the Earth. *Astronomy and Astrophysics* 428, 261-285, doi: 10.1051/0004-6361:20041335

Lawrence, K.T., Herbert, T.D., Brown, C.M., Raymo, M.E., Haywood, A.M., 2009. High-amplitude variations in North Atlantic sea surface temperature during the early Pliocene warm period. *Paleoceanography* 24, PA2218, doi: 10.1029/2008pa001669

Lawrence, K.T., Sosdian, S., White, H.E., Rosenthal, Y., 2010. North Atlantic climate evolution through the Plio-Pleistocene climate transitions. *Earth and Planetary Science Letters* 300, 329-342 doi: 10.1016/j.epsl.2010.10.013

Lisiecki, L.E., Raymo, M.E., 2005. A Pliocene-Pleistocene stack of 57 globally distributed benthic $\delta^{18}O$ records. *Paleoceanography* 20, PA1003, doi: 10.1029/2004PA001071

Lunt, D.J., Valdes, P.J., Haywood, A., Rutt, I.C., 2008. Closure of the Panama Seaway during the Pliocene: implications for climate and Northern Hemisphere glaciation. *Climate Dynamics* 30, 1-18, 10.1007/s00382-007-0265-6

Marincovich, L., Gladenkov, A.Y., 1999. Evidence for an early opening of the Bering Strait. *Nature* 397, 149-151, doi: 10.1038/16446

Marincovich, L., Gladenkov, A.Y., 2001. New evidence for the age of Bering Strait. *Quaternary Science Reviews* 20, 329-335, doi: 10.1016/S0277-3791(00)00113-X

Martinez-Boti, M.A., Foster, G.L., Chalk, T.B., Rohling, E.J., Sexton, P.F., Lunt, D.J., Pancost, R.D., Badger, M.P.S., et al., 2015. Plio-Pleistocene climate sensitivity evaluated using high-resolution CO_2 records. *Nature* 518, 49-54, doi: 10.1038/nature14145

Müller, P.J., Kirst, G., Ruhland, G., von Storch, I., Rosell-Melé, A., 1998. Calibration of the alkenone paleotemperature index $U^{K'}_{37}$ based on core-tops from the eastern South Atlantic and the global ocean (60 ^{o}N-60 ^{o}S). *Geochimica et Cosmochimica Acta* 62, 1757-1772, doi: 10.1016/S0016-7037(98)00097-0

Naafs, B.D.A., Hefter, J., Acton, G., Haug, G.H., Martínez-Garcia, A., Pancost, R., Stein, R., 2012a. Strengthening of North American dust sources during the late Pliocene (2.7 Ma). *Earth and Planetary Science Letters* 317-318, 8-19, doi: 10.1016/j.epsl.2011.11.026

Naafs, B.D.A., Hefter, J., Ferretti, P., Stein, R., Haug, G.H., 2011. Sea surface temperatures did not control the first occurrence of Hudson Strait Heinrich Events during MIS 16. *Paleoceanography* 26, PA4201, doi: 10.1029/2011PA002135

Naafs, B.D.A., Hefter, J., Grützner, J., Stein, R., 2013a. Warming of surface waters in the mid-latitude North Atlantic during Heinrich Events. *Paleoceanography* 28, 153-163, doi: 10.1029/2012PA002354

Naafs, B.D.A., Hefter, J., Stein, R., 2012b. Application of the long chain diol index (LDI) paleothermometer to the early Pleistocene (MIS 96). *Organic Geochemistry* 49, 83-85, doi: 10.1016/j.orggeochem.2012.05.011

Naafs, B.D.A., Hefter, J., Stein, R., 2013b. Millennial-scale ice rafting events and Hudson Strait Heinrich(-like) Events during the late Pliocene and Pleistocene: a review. *Quaternary Science Reviews* 80, 1-28, doi: 10.1016/j.quascirev.2013.08.014

Naafs, B.D.A., Stein, R., Hefter, J., Khèlifi, N., De Schepper, S., Haug, G.H., 2010. Late Pliocene changes in the North Atlantic Current. *Earth and Planetary Science Letters* 298, 434-442, doi: 10.1016/j.epsl.2010.08.023

O'Brien, C.L., Foster, G.L., Martinez-Boti, M.A., Abell, R., Rae, J.W.B., Pancost, R.D., 2014. High sea surface temperatures in tropical warm pools during the Pliocene. *Nature Geoscience* 7, 606-611, doi: 10.1038/ngeo2194

Otto-Bliesner, B.L., Jahn, A., Feng, R., Brady, E.C., Hu, A., Löfverström, M., 2017. Amplified North Atlantic warming in the late Pliocene by changes in Arctic gateways. *Geophysical Research Letters* 44, 957-964, doi: 10.1002/2016gl071805

Prahl, F.G., Wakeham, S.G., 1987. Calibration of unsaturation patterns in long-chain ketone compositions for palaeotemperature assessment. *Nature* 330, 367-369, doi: 10.1038/330367a0

Raymo, M.E., Hodell, D., Jansen, E., 1992. Response of Deep Ocean Circulation to Initiation of Northern Hemisphere Glaciation (3-2 MA). *Paleoceanography* 7, 645-672, doi: 10.1029/92pa01609

Robinson, M.M., Dowsett, H.J., Dwyer, G.S., Lawrence, K.T., 2008. Reevaluation of mid-Pliocene North Atlantic sea surface temperatures. *Paleoceanography* 23, PA3213, doi: 10.1029/2008pa001608

Rosell-Melé, A., Prahl, F.G., 2013. Seasonality of UK′37 temperature estimates as inferred from sediment trap data. *Quaternary Science Reviews* 72, 128-136, doi: 10.1016/j.quascirev.2013.04.017

Routson, C.C., McKay, N.P., Kaufman, D.S., Erb, M.P., Goosse, H., Shuman, B.N., Rodysill, J.R., Ault, T., 2019. Mid-latitude net precipitation decreased with Arctic warming during the Holocene. *Nature* 568, 83-87, doi: 10.1038/s41586-019-1060-3

Salzmann, U., Dolan, A.M., Haywood, A.M., Chan, W.-L., Voss, J., Hill, D.J., Abe-Ouchi, A., Otto-Bliesner, B., et al., 2013. Challenges in quantifying Pliocene terrestrial warming revealed by data-model discord. *Nature Climate Change* 3, 969-974, doi: 10.1038/nclimate2008

Schouten, S., Hopmans, E.C., Schefuss, E., Sinninghe Damsté, J.S., 2002. Distributional variations in marine crenarchaeotal membrane lipids: a new tool for reconstructing ancient sea water temperatures? *Earth and Planetary Science Letters* 204, 265-274, doi: 10.1016/S0012-821X(02)00979-2

Schreck, M., Meheust, M., Stein, R., Matthiessen, J., 2013. Response of marine palynomorphs to Neogene climate cooling in the Iceland Sea (ODP Hole 907A). *Marine Micropaleontology* 101, 49-67, doi: 10.1016/j.marmicro.2013.03.003

Seki, O., Foster, G.L., Schmidt, D.N., Mackensen, A., Kawamura, K., Pancost, R.D., 2010. Alkenone and boron-based Pliocene pCO_2 records. *Earth and Planetary Science Letters* 292, 201-211, doi: 10.1016/j.epsl.2010.01.037

Shackleton, N.J., Backman, J., Zimmerman, H., Kent, D.V., Hall, M.A., Roberts, D.G., Schnitker, D., Baldauf, J.G., et al., 1984. Oxygen isotope calibration of the onset of ice-rafting and history of glaciation in the North Atlantic region. *Nature* 307, 620-623, doi: 10.1038/307620a0

Shaw, T.A., Baldwin, M., Barnes, E.A., Caballero, R., Garfinkel, C.I., Hwang, Y.T., Li, C., O'Gorman, P.A., et al., 2016. Storm track processes and the opposing influences of climate change. *Nature Geoscience* 9, 656, doi: 10.1038/ngeo2783

Tierney, J.E., Tingley, M.P., 2014. A Bayesian, spatially-varying calibration model for the TEX_{86} proxy. *Geochimica et Cosmochimica Acta* 127, 83-106, doi: 10.1016/j.gca.2013.11.026

Tierney, J.E., Tingley, M.P., 2015. A TEX_{86} surface sediment database and extended Bayesian calibration. *Scientific Data* 2, 150029, doi: 10.1038/sdata.2015.29

Tierney, J.E., Tingley, M.P., 2018. BAYSPLINE: A New Calibration for the Alkenone Paleothermometer. *Paleoceanography and Paleoclimatology* 33, 281-301, doi: 10.1002/2017pa003201

Verhoeven, K., Louwye, S., Eiríksson, J., De Schepper, S., 2011. A new age model for the Pliocene–Pleistocene Tjörnes section on Iceland: Its implication for the timing of North Atlantic–Pacific palaeoceanographic pathways. *Palaeogeography, Palaeoclimatology, Palaeoecology* 309, 33-52, doi: 10.1016/j.palaeo.2011.04.001

Zhang, Y.G., Pagani, M., Liu, Z., 2014. A 12-Million-Year Temperature History of the Tropical Pacific Ocean. *Science* 344, 84-87, doi: 10.1126/science.1246172

Figure legend

Figure 1*; Modern-day SSTs and circulation in the North Atlantic. Location of sites discussed in this study are shown (Modified from De Schepper et al., 2013). NAC = North Atlantic Current.*

Figure 2*; Composite benthic foraminiferal* $\delta^{18}O$ *record from DSDP Site 610 (Jansen et al., 1988; Raymo et al., 1992; Kleiven et al., 2002; De Schepper et al., 2013, this study) – shown as single data points (red dots) and as 5 kyr moving averages (red line)– tuned to the LR04 global stack (Lisiecki and Raymo, 2005). Numbers and letter-number combinations indicate key glacial stages.*

Figure 3*; Benthic foraminiferal* $\delta^{18}O$ *record from DSDP Site 609 (Bartoli et al., 2005) – shown as single data points (red dots) and as 5 kyr moving averages (red line) – tuned to the LR04* *global stack (Lisiecki and Raymo, 2005). Numbers and letter-number combinations indicate key glacial stages.*

Figure 4*; Composite benthic foraminiferal $\delta^{18}O$ record from IODP Site U1313 (Bolton et al., 2010; De Schepper et al., 2013, this study) using our newly constructed age model – shown as single data points (red dots) and as 5 kyr moving averages (red line) – together with the LR04 global stack (Lisiecki and Raymo, 2005). Numbers and letter-number combinations indicate key glacial stages.*

Figure 5*; A) Composite benthic foraminiferal $\delta^{18}O$ record from DSDP Site 610 (blue line, 5 kyr moving average) with B) the alkenone- (orange circles), TEX_{86}-based (purple squares) SST records, and previously published G. bulloides Mg/Ca based SSTs (De Schepper et al., 2013; Hennissen et al., 2014; Karas et al., 2020). Thick lines in bottom panel represent 100 kyr moving averages. Inference of ice-rafter debris (IRD) occurrence at Site 610 from Kleiven et al. (2002). Timing of dinoflagellate turn-over at Site 610 from Hennissen et al. (2017). Uncertainty envelopes represent the combined analytical and calibration error for the U^{K}_{37}' and Mg/Ca-based SSTs and BAYSPAR calibration error for TEX_{86}-based SSTs.*

Figure 6*; A) Composite benthic foraminiferal $\delta^{18}O$ record (blue line, 5 kyr moving average) with B) the alkenone-based SST record from IODP Site U1313 (orange line). Thick line in bottom panel represent 100 kyr moving average. Ice-rafted debris (IRD) occurrence at Site U1313 following (Bailey et al., 2013; Naafs et al., 2013b). Timing of dinoflagellate turn-over at Site U1313 is based on the record from Hennissen et al. (2017). Uncertainty envelope represents the combined analytical and calibration error for the U^{K}_{37}'-based SSTs.*

***Figure 7**; A) Composite benthic foraminiferal $\delta^{18}O$ record (blue line) with B) the alkenone-based SST record from DSDP Site 609 (orange line). Uncertainty envelope represents the combined analytical and calibration error for the U^{K}_{37}'-based SSTs.*

***Figure 8;** A) summer insolation at 65 °N (Laskar et al., 2004), B) boron-based atmospheric CO_2 (orange; Seki et al., 2010; blue; Bartoli et al., 2011; green; Martinez-Boti et al., 2015), C) benthic $\delta^{18}O$ stack (Lisiecki and Raymo, 2005), D) 100 kyr moving average of the latitudinal SST gradient between 41 and 58 °N (Site U1313-982), and E) SST record of Sites U1313 (Naafs et al., 2010 and this study), 609 (Robinson et al., 2008 and this study), 610 (De Schepper et al., 2013 and this study), 982 (Lawrence et al., 2009), 642 (Bachem et al., 2017), and 907 (Herbert et al., 2016). SST uncertainty envelopes indicate the combined analytical (where available) and calibration error. Uncertainty for the CO_2 records are as in original papers.*

***Fig. 9;** A) Benthic $\delta^{18}O$ stack (Lisiecki and Raymo, 2005) for the period 4 – 2.5 Myr together with 100 kyr moving averages of B) latitudinal SST gradient Site U1313-982, and C) latitudinal SST gradients Site U1313-610 and the zonal SST gradient between Site 642-907.*

Supporting references

Bolton, C.T., Wilson, P.A., Bailey, I., Friedrich, O., Beer, C.J., Becker, J., Baranwal, S., Schiebel, R., 2010. Millennial-scale climate variability in the subpolar North Atlantic Ocean during the late Pliocene. *Paleoceanography* 25, PA4218, doi: 10.1029/2010PA001951

De Schepper, S., Groeneveld, J., Naafs, B.D.A., Van Renterghem, C., Hennissen, J., Head, M.J., Louwye, S., Fabian, K., 2013. Northern Hemisphere Glaciation during the Globally Warm Early Late Pliocene. *PLoS ONE* 8, e81508, doi: 10.1371/journal.pone.0081508

Expedition 306 Scientists, 2006. Site U1313, in: Channell, J.E.T., Kanamatsu, T., Sato, T., Stein, R., Alvarez Zarikian, C.A., Malone, M.J., Expedition 303/306 Scientists (Eds.), *Proceedings of Integrated Ocean Drilling Program* Integrated Ocean Drilling Program Management International, Inc., College Station TX.

Herbert, T.D., Schuffert, J.D., 1998. 2. Alkenone unsaturation estimates of late Miocene through late Pliocene sea-surface temperatures at Site 958, in: Firth, J.V. (Ed.), *Proceedings of the Ocean Drilling Program, Scientific Results, Vol. 159T*, pp. 17-21.

Jansen, E., Bleil, U., Henrich, R., Kringstad, L., Slettemark, B., 1988. Paleoenvironmental changes in the Norwegian Sea and the northeast Atlantic during the last 2.8 m.y.: Deep Sea Drilling Project/Ocean Drilling Program Sites 610, 642, 643 and 644. *Paleoceanography* 3, 563-581, doi: 10.1029/PA003i005p00563

Kleiven, H.F., Jansen, E., Fronval, T., Smith, T.M., 2002. Intensification of Northern Hemisphere glaciations in the circum Atlantic region (3.5-2.4 Ma) - ice-rafted detritus evidence. *Palaeogeography, Palaeoclimatology, Palaeoecology* 184, 213-223, doi: 10.1016/S0031-0182(01)00407-2

Lawrence, K.T., Herbert, T.D., Brown, C.M., Raymo, M.E., Haywood, A.M., 2009. High-amplitude variations in North Atlantic sea surface temperature during the early Pliocene warm period. *Paleoceanography* 24, PA2218, doi: 10.1029/2008pa001669

Naafs, B.D.A., Hefter, J., Stein, R., 2012. Application of the long chain diol index (LDI) paleothermometer to the early Pleistocene (MIS 96). *Organic Geochemistry* 49, 83-85, doi: 10.1016/j.orggeochem.2012.05.011

Naafs, B.D.A., Stein, R., Hefter, J., Khèlifi, N., De Schepper, S., Haug, G.H., 2010. Late Pliocene changes in the North Atlantic Current. *Earth and Planetary Science Letters* 298, 434-442, doi: 10.1016/j.epsl.2010.08.023

Raymo, M.E., Hodell, D., Jansen, E., 1992. Response of Deep Ocean Circulation to Initiation of Northern Hemisphere Glaciation (3-2 MA). *Paleoceanography* 7, 645-672, doi: 10.1029/92pa01609

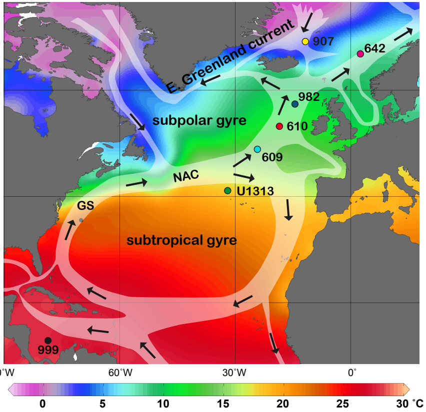
E. Greenland current
907
642
60°N
982
subpolar gyre
610
609
NAC
40°N
U1313
GS
subtropical gyre
20°N
999
90°W
60°W
30°W
0°
0
5
10
15
20
25
30 °C

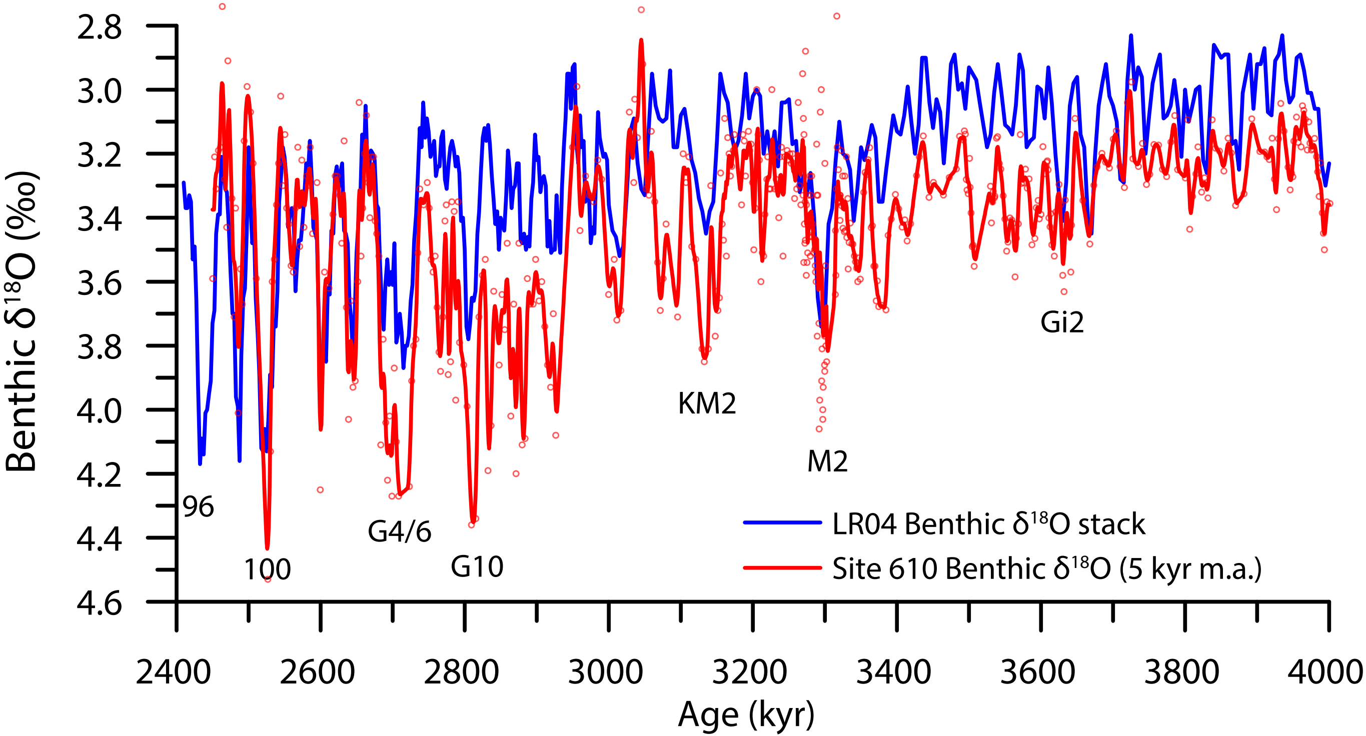

Benthic δ18O (‰)
2.8
3.0
3.2
3.4
3.6
3.8
4.0
4.2
4.4
4.6
96
100
G4/6
G10
KM2
M2
Gi2
LR04 Benthic δ18O stack
Site 610 Benthic δ18O (5 kyr m.a.)
2400
2600
2800
3000
3200
3400
3600
3800
4000
Age (kyr)

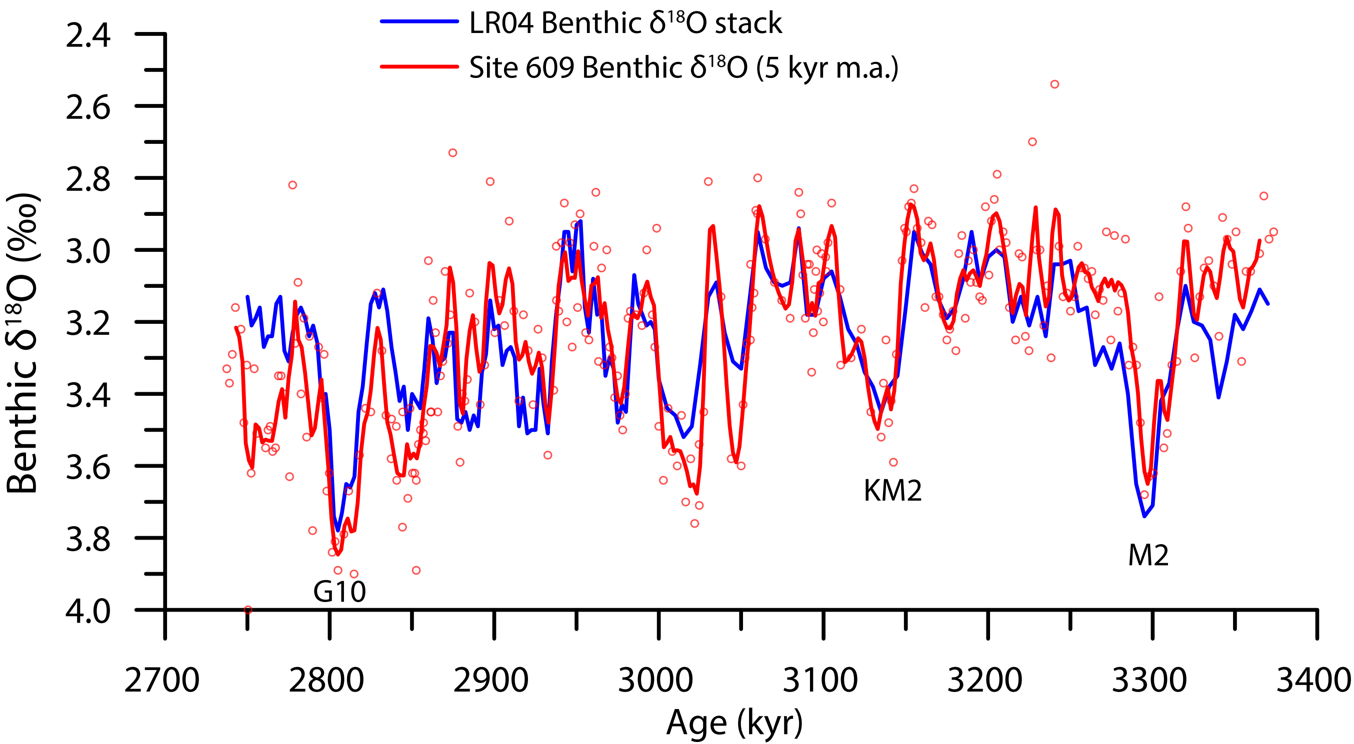

LR04 Benthic δ18O stack
Site 609 Benthic δ18O (5 kyr m.a.)
Benthic δ18O (‰)
2.4
2.6
2.8
3.0
3.2
3.4
3.6
3.8
4.0
G10
KM2
M2
2700
2800
2900
3000
3100
3200
3300
3400
Age (kyr)

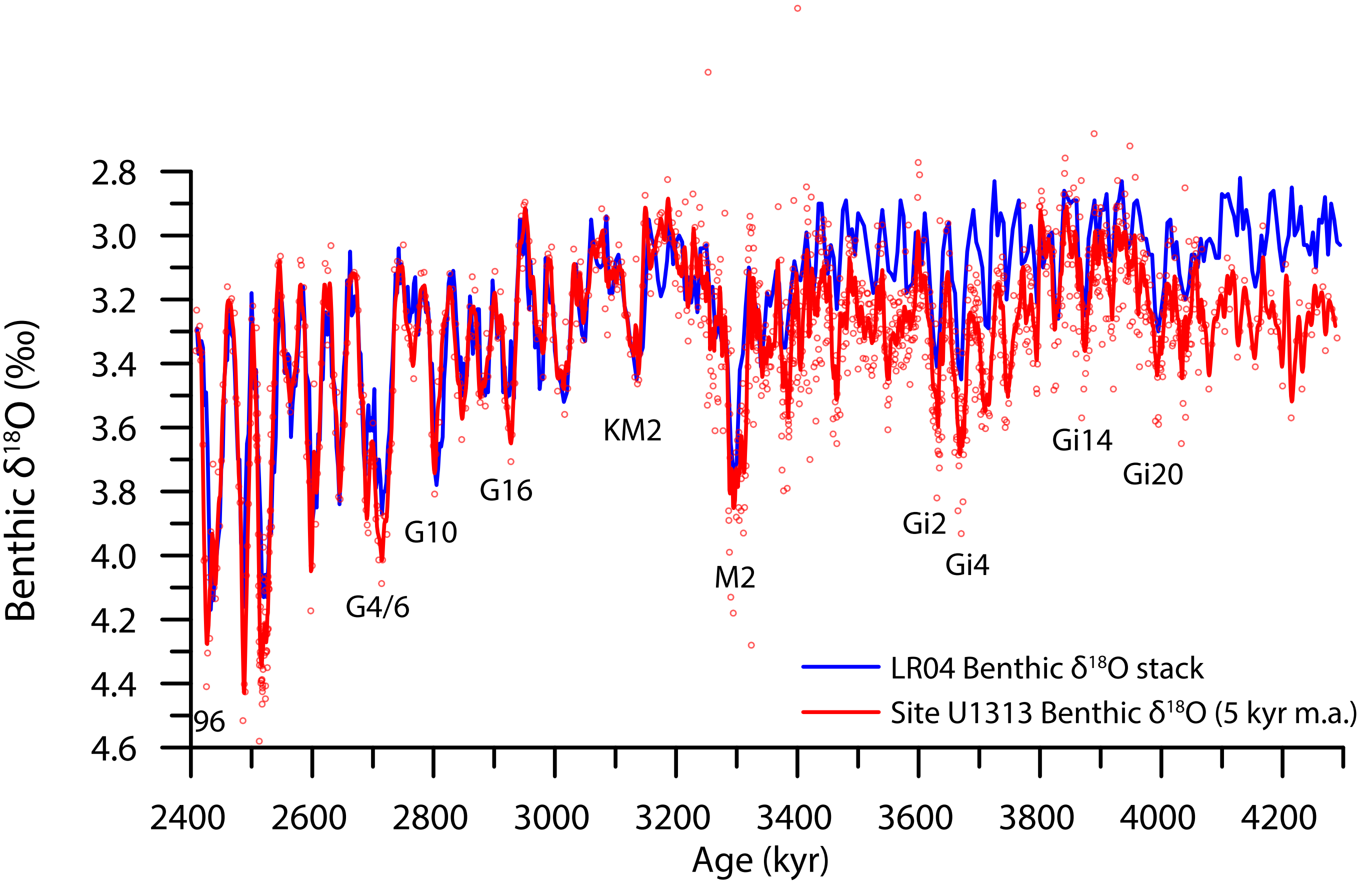

2.8
3.0
3.2
3.4
3.6
3.8
4.0
4.2
4.4
4.6
Benthic δ18O (‰)
96
G4/6
G10
G16
KM2
M2
Gi2
Gi4
Gi14
Gi20
LR04 Benthic δ18O stack
Site U1313 Benthic δ18O (5 kyr m.a.)
2400
2600
2800
3000
3200
3400
3600
3800
4000
4200
Age (kyr)

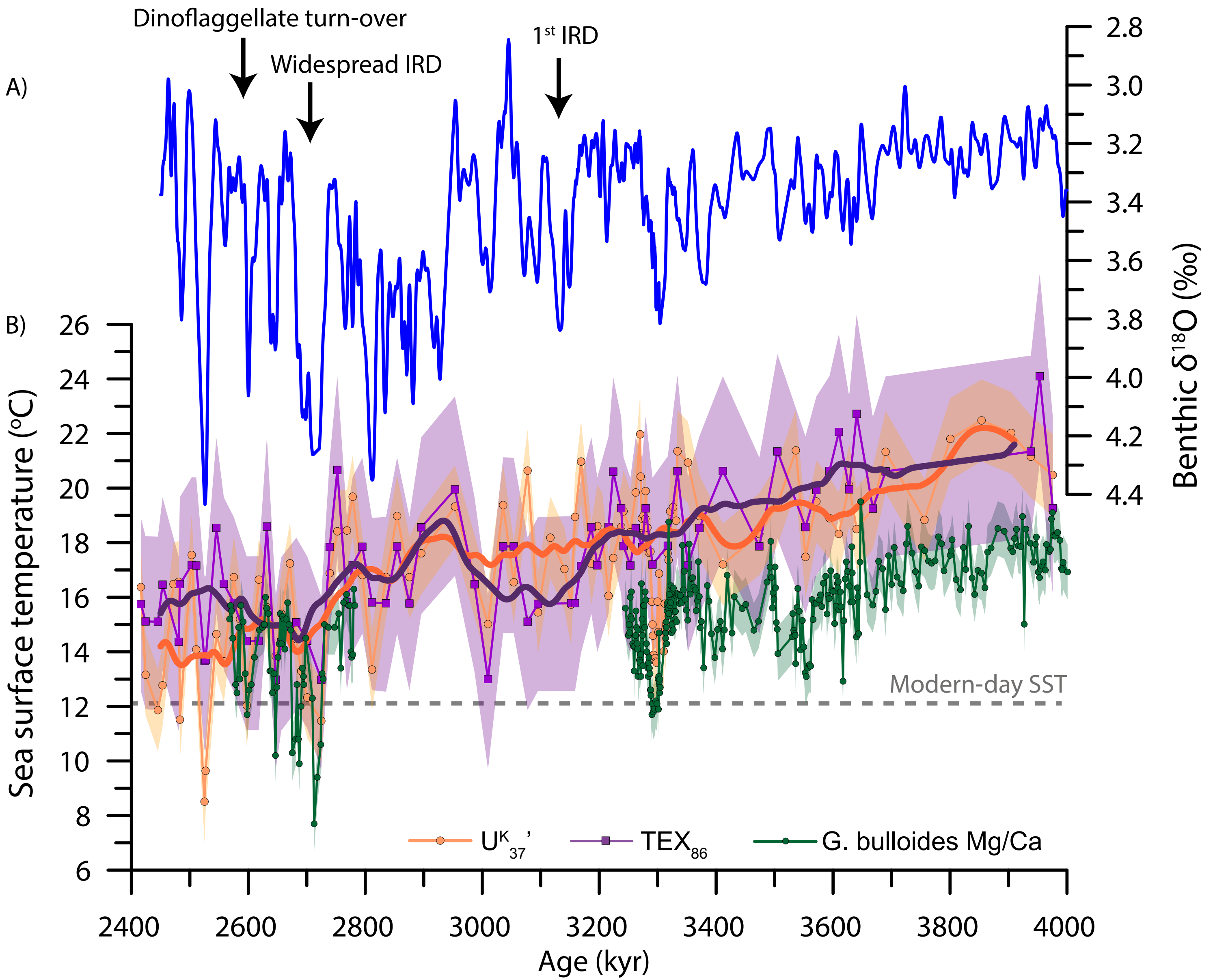

A)
B)
Dinoflaggellate turn-over
Widespread IRD
1st IRD
Benthic δ18O (‰)
2.8
3.0
3.2
3.4
3.6
3.8
4.0
4.2
4.4
Sea surface temperature (°C)
26
24
22
20
18
16
14
12
10
8
6
Modern-day SST
UK37'
TEX86
G. bulloides Mg/Ca
2400
2600
2800
3000
3200
3400
3600
3800
4000
Age (kyr)

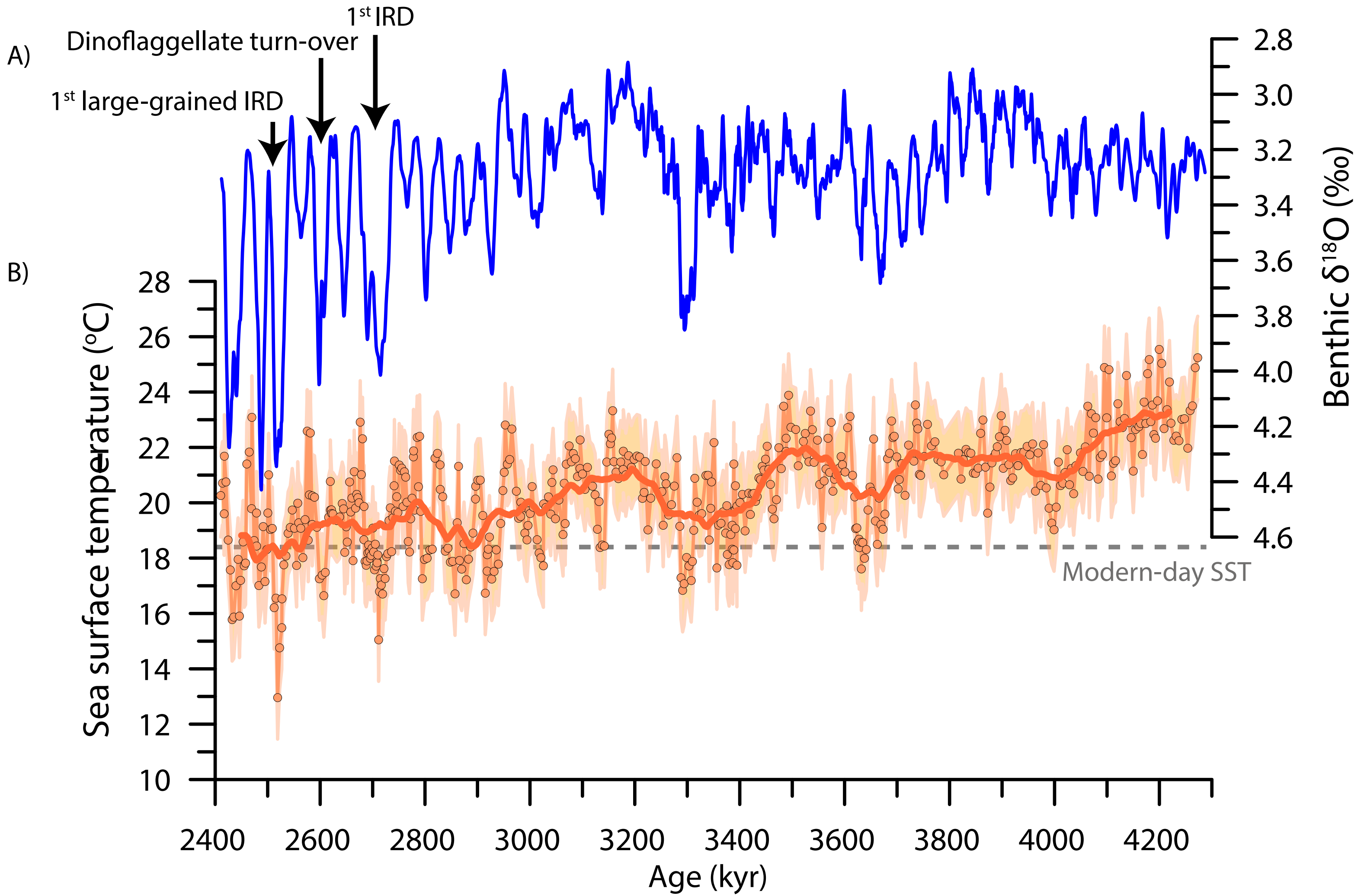

A)
B)
1st IRD
Dinoflaggellate turn-over
1st large-grained IRD
Benthic δ18O (‰)
2.8
3.0
3.2
3.4
3.6
3.8
4.0
4.2
4.4
4.6
Sea surface temperature (°C)
28
26
24
22
20
18
16
14
12
10
Modern-day SST
2400
2600
2800
3000
3200
3400
3600
3800
4000
4200
Age (kyr)

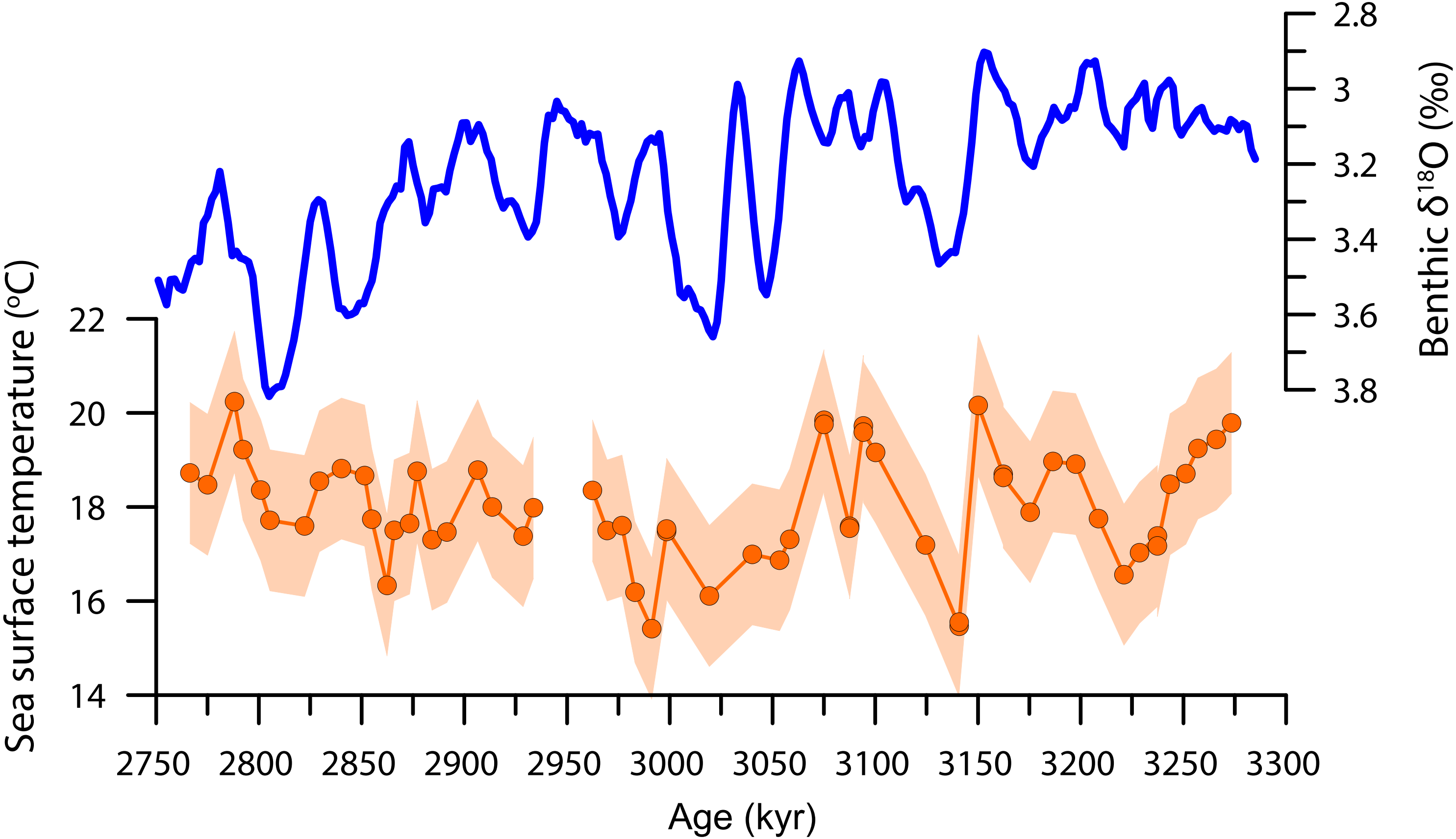

Sea surface temperature (°C)
22
20
18
16
14
Benthic δ18O (‰)
2.8
3
3.2
3.4
3.6
3.8
2750
2800
2850
2900
2950
3000
3050
3100
3150
3200
3250
3300
Age (kyr)

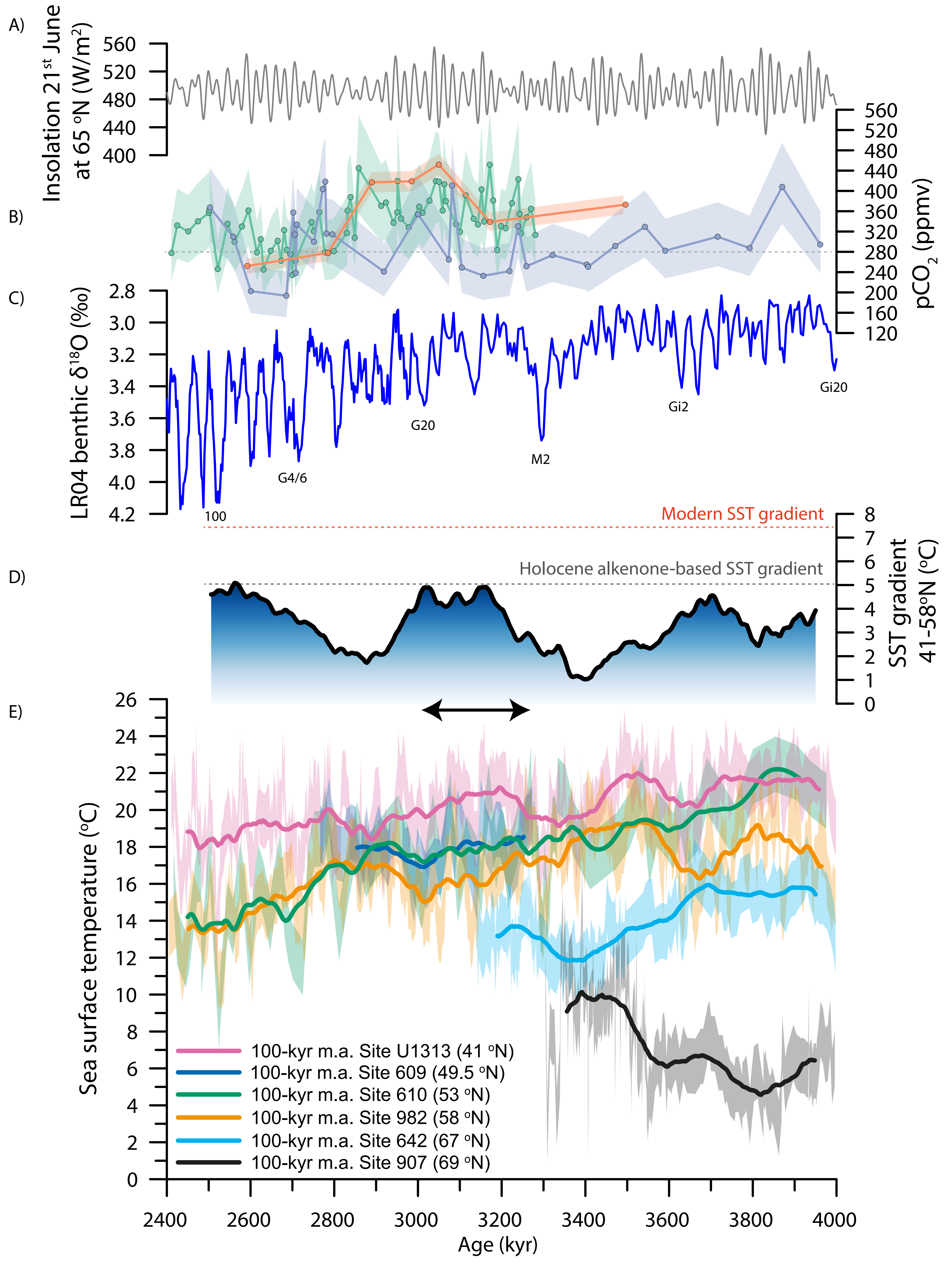

A)
Insolation 21st June at 65 °N (W/m2)
560
520
480
440
400
B)
pCO2 (ppmv)
560
520
480
440
400
360
320
280
240
200
160
120
C)
LR04 benthic δ18O (‰)
2.8
3.0
3.2
3.4
3.6
3.8
4.0
4.2
Gi20
Gi2
G20
M2
G4/6
100
Modern SST gradient
Holocene alkenone-based SST gradient
D)
SST gradient 41-58°N (°C)
8
7
6
5
4
3
2
1
0
E)
Sea surface temperature (°C)
26
24
22
20
18
16
14
12
10
8
6
4
2
0
100-kyr m.a. Site U1313 (41 °N)
100-kyr m.a. Site 609 (49.5 °N)
100-kyr m.a. Site 610 (53 °N)
100-kyr m.a. Site 982 (58 °N)
100-kyr m.a. Site 642 (67 °N)
100-kyr m.a. Site 907 (69 °N)
2400
2600
2800
3000
3200
3400
3600
3800
4000
Age (kyr)

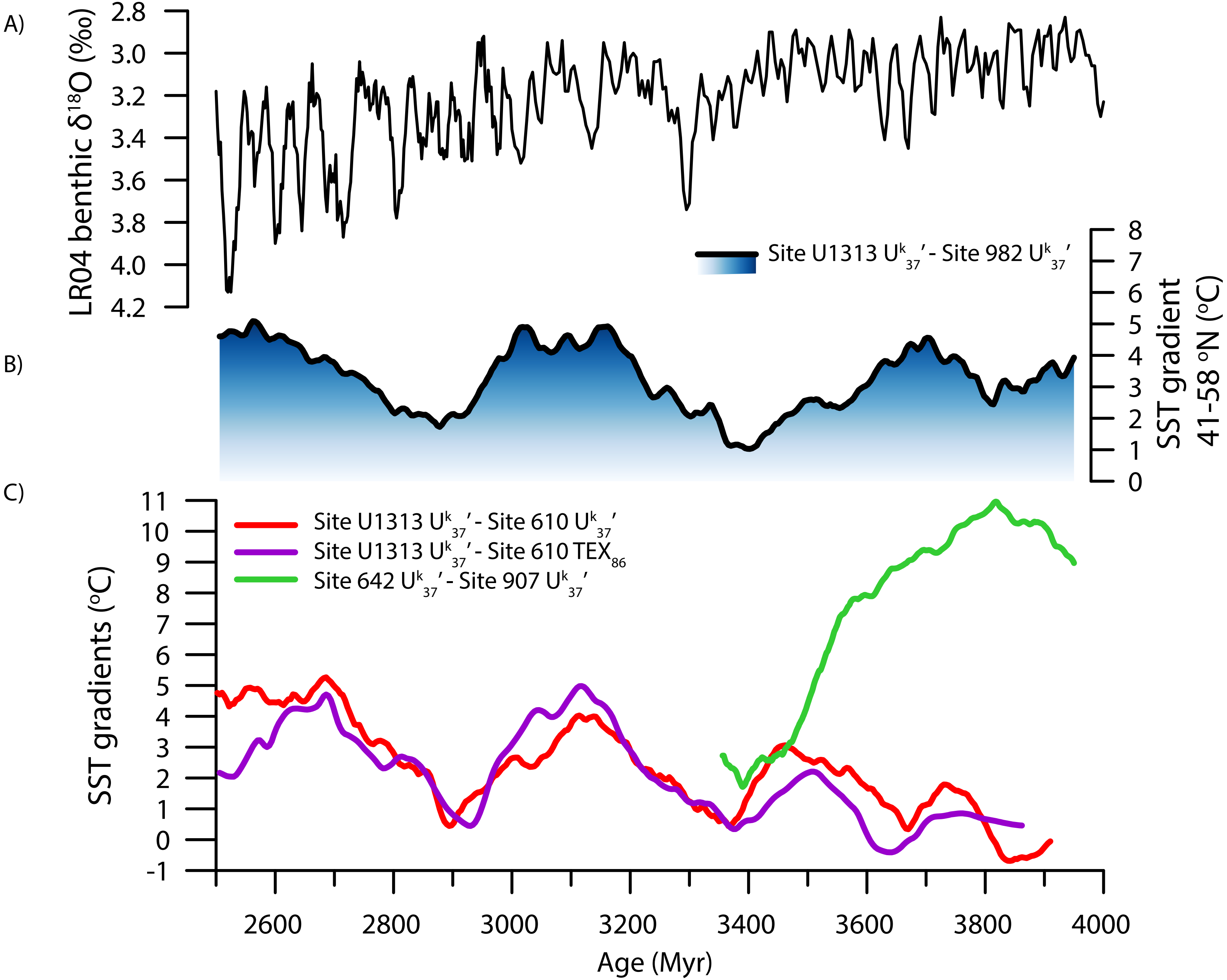

A)
LR04 benthic $\delta^{18}O$ (‰)
2.8
3.0
3.2
3.4
3.6
3.8
4.0
4.2
Site U1313 U^k_{37}′ - Site 982 U^k_{37}′
B)
SST gradient 41-58 °N (°C)
8
7
6
5
4
3
2
1
0
C)
Site U1313 U^k_{37}′ - Site 610 U^k_{37}′
Site U1313 U^k_{37}′ - Site 610 TEX_{86}
Site 642 U^k_{37}′ - Site 907 U^k_{37}′
SST gradients (°C)
11
10
9
8
7
6
5
4
3
2
1
0
-1
2600
2800
3000
3200
3400
3600
3800
4000
Age (Myr)

Paleoceanography and Climatology

Supporting Information for

Repeated near-collapse of the Pliocene sea surface temperature gradient in the North Atlantic

B.D.A. Naafs[1,2], A.H.L. Voelker[3,4], C. Karas[5,6,7,8], N. Andersen[9], F.J. Sierro[10]

[1]Organic Geochemistry Unit, School of Chemistry and Cabot Institute, University of Bristol, Bristol, UK
[2]School of Earth Sciences, University of Bristol, Bristol, UK
[3]Divisão de Geologia e Georecursos Marinhos, Instituto Português do Mar e da Atmosfera, Lisboa, Portugal
[4]CCMAR, Centro de Ciências do Mar, Universidade do Algarve, Campus de Gambelas, Faro, Portugal
[5]Goethe-University Frankfurt, Altenhoeferallee 1, 60438, Frankfurt am Main, Germany
[6]Lamont-Doherty Earth Observatory, Geoscience, Palisades, USA
[7]Instituto de Geografía, Pontificia Universidad Católica de Chile, Santiago, Chile
[8]Millennium Nucleus Paleoclimate, University of Chile, Santiago, Chile
[9]Leibniz Laboratory for Radiometric Dating and Stable Isotope Research, CAU Kiel, Kiel, Germany
[10]Department of Geology, Faculty of Sciences, University of Salamanca, Salamanca, Spain

Contents of this file

Figures S1 to S4

Additional Supporting Information (Files uploaded separately)

None

Introduction

This file contains four supplementary figures.

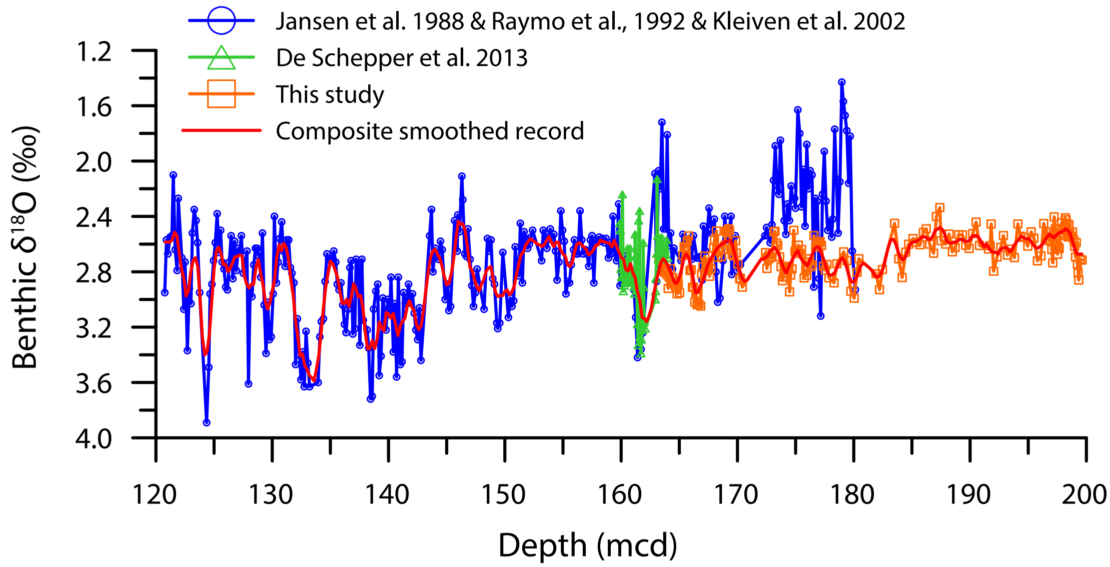

Figure S1; All available uncorrected benthic foraminiferal $\delta^{18}O$ from DSDP Site 610 versus depth (Jansen et al., 1988; Raymo et al., 1992; Kleiven et al., 2002; De Schepper et al., 2013, this study).

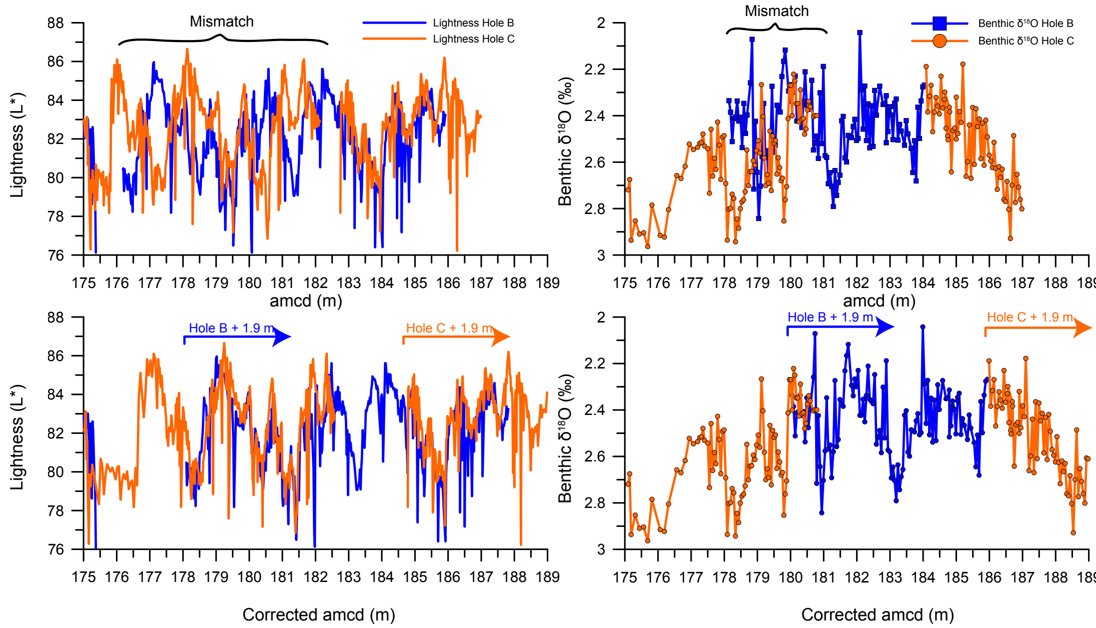

Figure S2; *Primary splice correction for Site U1313 between 176 and 183 amcd demonstrated by the lightness (L*) (Expedition 306 Scientists, 2006) and benthic foraminiferal $\delta^{18}O$ records for Holes U1313B and U1313C (this study).*

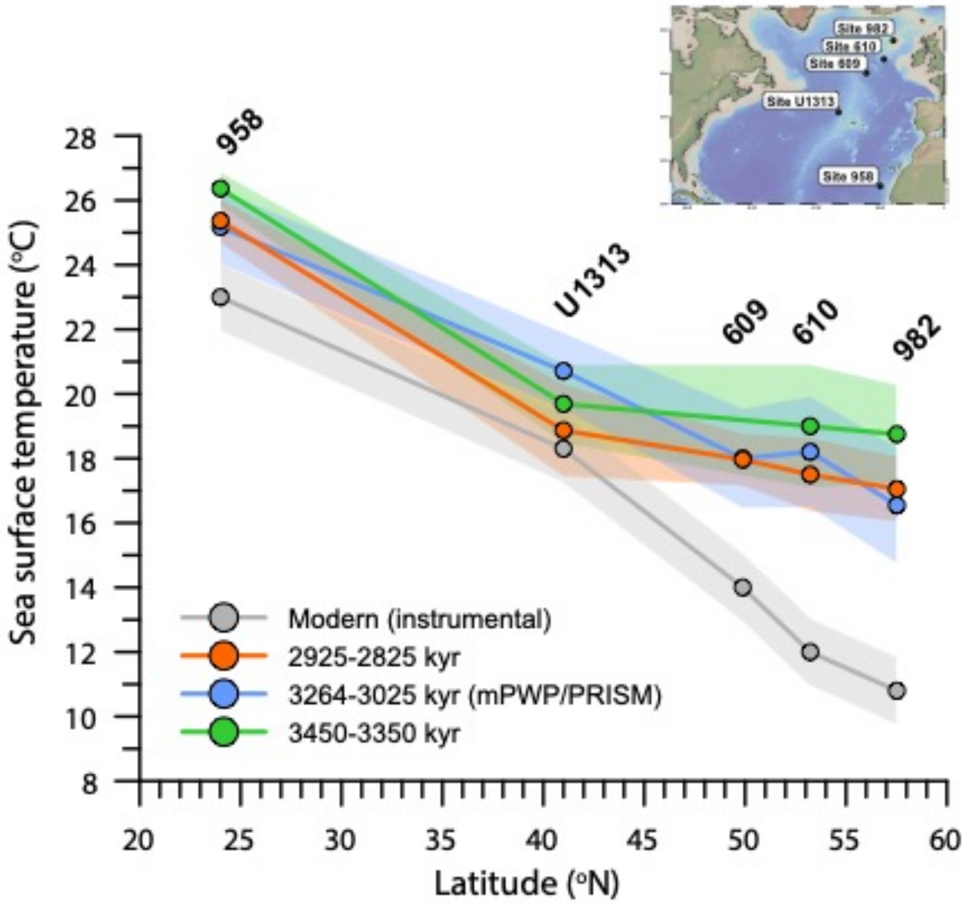

Figure S3; *Average alkenone-based SST across the (mid-latitude) North Atlantic for the two periods characterized by a near-collapse of the SST gradient (3.45-3.35 and 2.925-2.825 Myr), as well as the gradient during the mPWP/PRISM interval (3.264-3.025 Myr) and the modern instrumental gradient (grey). Data from Site 982 is from (Lawrence et al., 2009). Data from Site 958 is from (Herbert and Schuffert, 1998).*

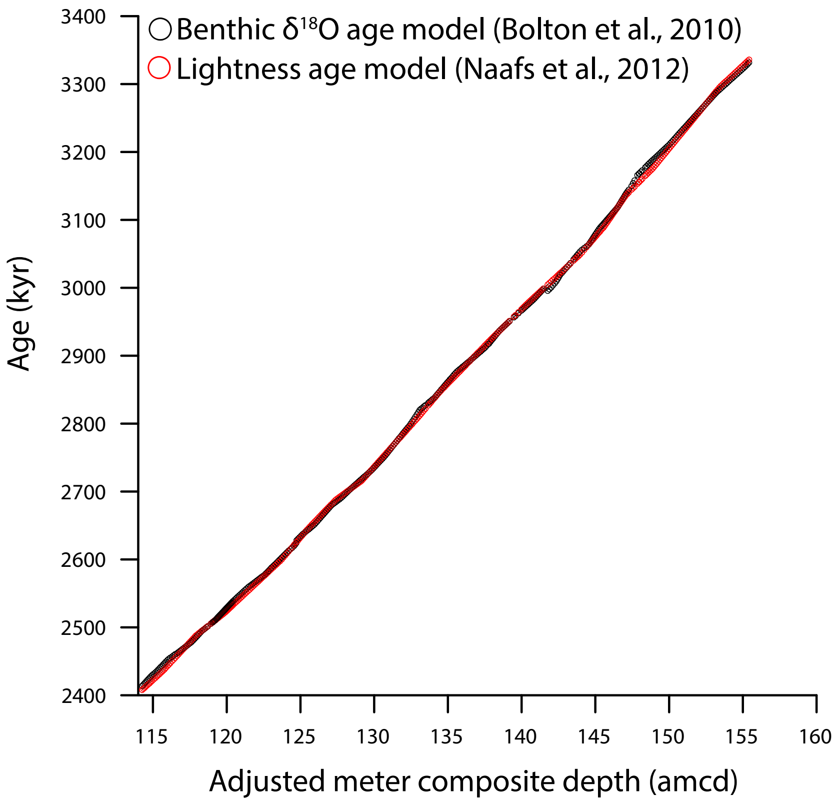

Figure S4; *Comparison of the benthic foraminiferal $\delta^{18}O$ based age model for Site U1313* ***(Bolton et al., 2010) and that based on the lightness of Site U1313 (Naafs et al., 2010; Naafs et al., 2012).***

Supporting references

Bolton, C.T., Wilson, P.A., Bailey, I., Friedrich, O., Beer, C.J., Becker, J., Baranwal, S., Schiebel, R., 2010. Millennial-scale climate variability in the subpolar North Atlantic Ocean during the late Pliocene. *Paleoceanography* 25, PA4218, doi: 10.1029/2010PA001951

De Schepper, S., Groeneveld, J., Naafs, B.D.A., Van Renterghem, C., Hennissen, J., Head, M.J., Louwye, S., Fabian, K., 2013. Northern Hemisphere Glaciation during the Globally Warm Early Late Pliocene. *PLoS ONE* 8, e81508, doi: 10.1371/journal.pone.0081508

Expedition 306 Scientists, 2006. Site U1313, in: Channell, J.E.T., Kanamatsu, T., Sato, T., Stein, R., Alvarez Zarikian, C.A., Malone, M.J., Expedition 303/306 Scientists (Eds.), *Proceedings of Integrated Ocean Drilling Program* Integrated Ocean Drilling Program Management International, Inc., College Station TX.

Herbert, T.D., Schuffert, J.D., 1998. 2. Alkenone unsaturation estimates of late Miocene through late Pliocene sea-surface temperatures at Site 958, in: Firth, J.V. (Ed.), *Proceedings of the Ocean Drilling Program, Scientific Results, Vol. 159T*, pp. 17-21.

Jansen, E., Bleil, U., Henrich, R., Kringstad, L., Slettemark, B., 1988. Paleoenvironmental changes in the Norwegian Sea and the northeast Atlantic during the last 2.8 m.y.: Deep Sea Drilling Project/Ocean Drilling Program Sites 610, 642, 643 and 644. *Paleoceanography* 3, 563-581, doi: 10.1029/PA003i005p00563

Kleiven, H.F., Jansen, E., Fronval, T., Smith, T.M., 2002. Intensification of Northern Hemisphere glaciations in the circum Atlantic region (3.5-2.4 Ma) - ice-rafted detritus evidence. *Palaeogeography, Palaeoclimatology, Palaeoecology* 184, 213-223, doi: 10.1016/S0031-0182(01)00407-2

Lawrence, K.T., Herbert, T.D., Brown, C.M., Raymo, M.E., Haywood, A.M., 2009. High-amplitude variations in North Atlantic sea surface temperature during the early Pliocene warm period. *Paleoceanography* 24, PA2218, doi: 10.1029/2008pa001669

Naafs, B.D.A., Hefter, J., Stein, R., 2012. Application of the long chain diol index (LDI) paleothermometer to the early Pleistocene (MIS 96). *Organic Geochemistry* 49, 83-85, doi: 10.1016/j.orggeochem.2012.05.011

Naafs, B.D.A., Stein, R., Hefter, J., Khèlifi, N., De Schepper, S., Haug, G.H., 2010. Late Pliocene changes in the North Atlantic Current. *Earth and Planetary Science Letters* 298, 434-442, doi: 10.1016/j.epsl.2010.08.023

Raymo, M.E., Hodell, D., Jansen, E., 1992. Response of Deep Ocean Circulation to Initiation of Northern Hemisphere Glaciation (3-2 MA). *Paleoceanography* 7, 645-672, doi: 10.1029/92pa01609